Field evidence for substrate entrainment by pyroclastic density currents and its effect on downstream dynamics at Mount St Helens, Washington (USA)

Nicholas M. Pollock

A Thesis submitted in partial fulfillment of the requirements for the degree of

Master of Science

University of Washington

2013

Committee:

Brittany Brand
George Bergantz
Darrel Cowan

Program Authorized to Offer Degree:

Earth and Space Sciences

Table of Contents

Abstract……5

Chapter 1…….. 6
1.1 Aim…… 6
1.2 Introduction……... 6
1.3 Generation of Pyroclastic Density Currents…….. 7
1.4 Flow Regimes…….. 10
1.5 Erosion by PDCs…… 20

Chapter 2…… 23
2.1 Introduction…… 23
2.2 May 18th 1980 Eruption at Mount St Helens…….. 25
2.3 Methods…….. 28
2.3.1 Field Methods…… 28
2.3.2 Chi-Square Test for Homogeneity…… 29
2.4 Results…… 31
2.4.1 Fall Deposits……... 31
2.4.2 Debris Avalanche Hummocks…… 32
2.4.3 Pyroclastic Density Current Deposits…… 33
2.4.4 Interpretation of Results…… 49
2.4.5 Interpretation of Channelization Features…….. 53
2.5 Discussion……54
2.5.1 Conditions Promoting Erosion……54
2.5.1.1 Effects of Velocity and Acceleration……54
2.5.1.2 Effects of Surface Roughness……55
2.5.2 Mechanisms of Substrate Entrainment……... 56
2.5.3 Effects of Channelization……59
2.6 Conclusions…… 60

List of Figures

Figure 1—DEM of Mount St Helens with Sample Locations……25

Figure 2—Componentry of the Fall Deposits……..31

Figure 3—Outcrop C-1: Diagram and Componentry…….. 34

Figure 4—Outcrop B-3: Diagram Componentry……35

Figure 5—Outcrop B-3: Granulometry……37

Figure 6—Outcrop X-2: Diagram and Componentry……..38

Figure 7—Outcrop X-2: Granulometry……39

Figure 8—Outcrop X-2: Granulometry with Height Above Base……...40

Figure 9—Outcrop T-2: Diagram and Componentry…….. 41

Figure 10—Outcrop T-2: Granulometry……. 42

Figure 11—Outcrop AD-2a: Diagram and Componentry……... 44

Figure 12—Outcrop D-4: Diagram and Componentry……....46

Figure 13—Outcrop AD-3b: Diagram and Componentry……...47

List of Tables

Table 1—Chi Square example set up…….. 30

Table 2—Full data set……..69

Abstract

Despite recent advances in the study of pyroclastic density current (PDC) dynamics, several fundamental aspects of the behavior of these hazardous currents remain poorly understood. Perhaps two of the more significant gaps in our knowledge are the primary control(s) on substrate erosion and the effect that substrate entrainment, i.e. bulking, has on current dynamics. Perhaps the largest limitation to a comprehensive investigation into this topic previously was the lack of sufficient exposures to confidently identify depositional evidence for substrate entrainment, the source of entrained blocks, and the effect on downstream flow dynamics. However, more than thirty years of erosion into the May 18, 1980 PDC and debris avalanche hummock deposits at Mount St Helens has revealed kilometers of new outcrops containing substantial evidence for erosion and entrainment. Here we present evidence for the entrainment of lithic blocks (>1 m in diameter in some locations) from the debris avalanche hummocks, as determined through detailed componentry and granulometry. We find that in locations where local substrate entrainment has occurred there is an increase in median grain size, an increase in fine ash, a decrease in the pumice to lithic ratio, and an increase in lithologies present in the upstream debris avalanche hummocks. We also observe numerous scours filled with block-rich lithic facies downstream from hummocks where lithic plucking has been determined. This observation suggests that erosion is a self-perpetuating process; when substrate entrainment occurs the increased bulk density and concentration gradient that result in the current enables further erosion and entrainment downstream from the location where bulking initially occurred. In addition, the presence of large, locally entrained lithics at various heights within a single flow unit suggests both a progressive entrainment of the substrate as well as a progressive aggradation of the deposit, depending on localized flow conditions. However, as the hummocks were progressively filled in during the eruption, the amount of entrained substrate material decreased to zero, suggesting that surface roughness is important for promoting erosion by PDCs. Taken together, these results suggest that the incorporation of substrate material by PDCs has a significant impact on PDC dynamics and deserves to be investigated further. It is possible that with the combination of field investigations, laboratory experiments, and numerical modeling a more complete understanding of how erosion and entrainment affect PDC dynamics can lead to a more accurate hazard assessment for these dangerous currents.

Chapter 1

1.1 Aim

The goal of this work is to describe field evidence for substrate entrainment by pyroclastic density currents from the May 18, 1980 eruption at Mount St Helens (Washington, USA). Included will be a discussion on the conditions under which erosion is favored and how the current is subsequently affected by entrainment. The goal of this literature review is to provide the foundation of research that has informed our state of knowledge regarding the processes operating within a range of granular flows, to determine where gaps in our knowledge exist, and to identify which remaining questions we will address with our research objectives.

1.2 Introduction

Pyroclastic density currents (herein referred to as PDCs) are heterogeneous mixtures of volcanic gases, ash, and rock that travel down-slope because their density is greater than that of the ambient environment (Branney and Kokelaar, 2002). This definition intentionally covers a wide spectrum of flow types and conditions, from the dilute to the highly concentrated. PDCs can be generated by a number of mechanisms, as will be discussed below, and the resulting deposits often reflect the manner in which the current was generated.

Many classification schemes have been developed to describe PDCs, but the two most prominent are the Williams (1957) system and that of Branney and Kokelaar (2002). The Williams classification scheme is based on observations of past eruptions at a number of volcanoes. The benefit to this method of classification is that it allows for deposits from extinct volcanoes to be compared to modern analogues in order to facilitate visualization of the style of

eruption. The disadvantage to this scheme is that it is based on a limited number of observed volcanic eruptions, and trying to place modern eruptions and/or newly described outcrops into the context of only a few past eruptions is not always possible because in reality PDCs occur within a continuum.

In contrast, the Branney and Kokelaar classification scheme is based on the mechanism by which the PDC was generated and allows the styles of PDC to more easily grade into one another. For this reason this is the system that will be further discussed and used throughout the remainder of this work.

1.3 Generation of Pyroclastic Flows

PDCs are formed by a variety of mechanisms and can vary by many orders of magnitude in both size and duration. Durations of PDC transport can vary from seconds up to hours and the resulting deposits can range from thousands of cubic meters to thousands of cubic kilometers. PDCs produced by each of these different mechanisms will be inherently different from those produced by others in their concentration, bulk density, componentry, temperature and velocity. Because of these different flow characteristics, the transport, depositional, and erosional tendencies may be very different for currents generated by different mechanisms.

1.3.1 Type A: Single Pulse Column Collapse

During the course of an explosive eruption, such as phreatomagmatic, Vulcanian, Sub-Plinian, or Plinian eruptions, the eruptive conditions at the vent may change such that either a momentary instability or spatial heterogeneity is produced that allows for the initiation of a PDC. These instabilities can be caused by a decrease in either the mass flux of eruptive material or

eruption velocity and by a widening of the conduit due to vent erosion (Freundt and Bursik, 1998). In addition, if the column cannot ingest enough cold, ambient air, the column (or parts of it) may cease to remain buoyant and collapse back towards the surface (Dobran et al., 1993). PDCs that are produced due to column collapse tend to form fines-rich ignimbrites due to the efficient magmatic fragmentation deep in the conduit and comminution of pumice during rapid ascent within the conduit. This type of pyroclastic flow has been generated at Novarupta in 1912 (Fierstein and Hildreth, 1992) and Mt Pinatubo in 1991 (Scott et al., 1996), among many others.

1.3.2 Type B: Sustained Fountaining from Plinian Column

When only one region within a Plinian column collapses, it is possible that that region continues to feed the PDCs. This steadiness at the vent allows for continuous feeding of the PDCs for durations that can last up to hours and produce ignimbrites thousands of cubic kilometers in size. The largest ignimbrites ever produced are thought to have formed in this manner. For example, the Bishop and Bandalier tuffs are over 600 and 400 cubic kilometers in volume, respectively, and are believed to have been emplaced over approximately 28 hours (Bursik and Woods, 1996).

1.3.3 Type C: Sustained Low Fountaining

This type of PDC forming mechanism is transitional from the sustained fountaining mechanism. The only difference between the two is the presence of a sustained eruptive column for the duration of the previous mechanism, while a somewhat transient eruptive column characterizes sustained low fountaining. PDCs of this type are said to have “boiled-over” the crater rim as the material never lofted into the eruption column, but rather it spilled over the

ramparts. PDCs emplaced during the afternoon of May 18, 1980 at Mount St Helens were generated by this low fountaining, boiling-over mechanism (Hoblitt, 1980; Rowley et al., 1981). It is possible that a single volcanic eruption (or even a single ignimbrite) transitions from Type B to Type C.

1.3.4. Type D: Single Pulse Lateral Blast

Occasionally vent geometry will result in an inclined or laterally directed eruption column, perhaps the most notable example being the initial lateral blast that occurred during the May 18, 1980 eruption at Mount St Helens (Druitt, 1992). PDCs of this type may at first be dominated by inertial effects due to overpressure in the vent, but eventually transition to traditional gravity dominated PDCs (Belousov et al., 2007; Espoti Ongaro et al., 2012). The historically observed eruptions that produced PDCs of this type were of small volume and only erupted over a short period of time.

1.3.5 Type E: Gravitational Dome Collapse

When a lava dome or lava flow front becomes over-steepened it will often collapse, resulting in a PDC. As the dome front fails, clast comminution and vesicle rupture rapidly occur along with the admixing of ambient air resulting in expansion of the flow. Deposits from PDCs generated by dome collapse frequently contain a much higher proportion of large lithic blocks than PDCs generated by column collapse. These blocks are pieces of the dome that are incorporated into the flow and then transported down-slope. This type of PDC generation is common at Santiaguito (Rose et al., 1987), Merapi, (Beardintzeff, 1984), Mount Unzen (Yamamoto, 1993), and Montserrat (Cole et al., 1998; 2002).

1.3.6 Type F: Secondary Collapse of Ignimbrites

An ignimbrite, once emplaced, can remain highly mobile due to the trapping of gases within the deposit itself. This results in a fluid-like nature of the deposits and can result in secondary PDCs when collapse of the ignimbrite occurs along unstable surfaces. Secondary PDCs of this nature tend to occur within hours to days after the eruption. There is another type of secondary PDC in which erosion through the deposits creates an over-steepening of the unconsolidated ignimbrite. When the ignimbrite fails, the deposit can then be remobilized as secondary PDCs. This type of event can occur years after the initial eruption. Secondary collapse PDCs have been observed at Mount Pinatubo (Torres et al., 1996) and Mount St Helens (Brantley and Waitt, 1988).

1.4 Flow Regimes

There are three main, end-member flow regimes in which PDCs can be transported: granular (e.g. Denlinger, 1987; Dobran et al., 1993), turbulent (e.g. Valentine, 1987), and fluidized to semi-fluidized (e.g. Sparks, 1976; Wilson 1980). This next section details how each flow regime varies in particle support, transport and depositional mechanisms, and how these influence flow mobility and the ability of each type of flow to erode the substrate. It is important to note that the resulting deposits reflect only the conditions in the basal portion of the current just prior to deposition (Branney and Kokelaar, 2002). They give little information about the processes by which the flow was transported prior to the point of deposition, only how the current was behaving at the point of deposition. Also, these flow regimes exist within a continuum, and it is possible for even a single pulse flow to transition rapidly between them.

These rapid flow regime changes may result in vastly different depositional characteristics over a small spatial area (Branney and Kokelaar, 2002).

1.4.1 Granular Flow

Granular flow becomes the dominant flow regime in highly concentrated flows when the interstitial fluid does not influence the individual motion of particles. This flow regime is typical of mass wasting events such as rock falls and avalanches. In these rapidly shearing granular masses, it is the solid grain collisions that allow for the downslope transfer of mass and momentum (Campbell, 1990). The frequency with which these collisions occur is termed the *granular temperature,* which is analogous to the motion of molecules in kinetic gas theory (Ogawa, 1978; Savage 1983, 1984). However, because the collisions are inelastic, the granular temperature cannot be maintained indefinitely and high shear rates within the granular mass are required to sustain high granular temperatures (Campbell and Brennen, 1985). Thus the high shear rates in the flow, the higher the granular temperature. Granular temperature is important for particle support and particle segregation in granular flows, which will be discusses in the following sections.

True granular flow, in which the effects of the interstitial fluid are not important, is not likely to occur in PDCs because of the mixture of volcanic gases and fine ash particles that exists nearly ubiquitously between the larger clasts. Instead, it is more likely that these currents exist as a *modified granular flow* where the interstitial fluid influences flow properties and behaviors (Lowe, 1982). This modified granular flow-type behavior grades into semi-fluidized behavior, which will be discussed in Section 1.4.3.

1.4.1.1 Particle Support

It is possible for a current with a high granular temperature to maintain a liquefied state due to the *dispersive pressure* (Bagnold, 1954). Dispersive pressure is the term for the pressure associated with granular temperature that forces particles apart from one another due to clast collisions and results in dilation of the flow. Because it is directly related to the granular temperature, dispersive pressure is maximized when shear rates within the current are maximized (Lowe, 1982; Campbell, 1990). Dispersive pressure also acts to increase the mobility of granular flows due to expansion, which effectively decreases its viscosity (Lowe, 1976)

1.4.1.2 Particle Segregation

Dispersive pressure has also been invoked as a method by which inverse grading may occur in shearing granular masses. Bagnold (1954) suggests that shear-rate gradients develop within these currents, and dispersive pressure forces larger grains to regions of lower shear stress. In a granular flow, the region of the current where shear stresses are minimized is the upper free surface of the current, resulting in the reorganization of large clasts to the upper portions of the current. Thus, if the deposit aggrades rapidly enough, this inverse grading of clasts would be preserved in the deposit. *Kinetic sieving* occurs when smaller grains percolate down through space between larger clasts, again resulting in the upward migration of large clasts and inverse grading (Savage and Lun, 1988). In addition, there may be a *surface-roughness effect* whereby large grains are able to roll over smaller grains, but smaller grains cannot overpass large grains. This over-passing of large grains eventually results in smaller clasts settling towards the base of the current, and large clasts occupying the upper portions of the concentrated part of the flow (Nemec, 1990). All three of these mechanisms, however, neglect

the fact that PDCs are polydisperse mixtures in which both size and density can vary greatly. These mechanisms account for inverse grading in mixtures of equal density, but they ignore the buoyancy effects that would exist in a current consisting of clasts of varying density (Branney and Kokelaar, 2002). These buoyancy effects would force large clasts with low density towards the upper portions of the current differently than they would large clasts of high density. Branney and Kokelaar (2002) recognize the significant need for more work to reconcile both the mechanical and buoyant processes that may result in clast segregation.

1.4.1.3 Deposition

Deposition from the granular flow regime mainly occurs due to frictional freezing. This process occurs as clasts at the base of the current come to a halt due to frictional interlocking with the substrate. The clasts do not deposit individually, but rather they come to rest when they interlock with nearby particles (Hein, 1982; Hiscott, 1994). The highly concentrated nature of the current at the point of deposition results in little to no clast segregation at the flow boundary, but clast segregation may be important at higher levels within the current. This process occurs from the base of the current and migrates upwards (Branney and Kokelaar, 2002). The high granular temperatures that exist at the base of the current due to the high concentration of particles and high shear rates may cause dilation of the uppermost surface of the deposit. This dilation can result in a diffuse flow boundary in which the border between what is the deposit and what is in the current is not clear (Savage, 1979).

1.4.1.4 Resulting Deposits

Deposits from granular flow tend to be massive, and relatively structureless due to the rapid deposition and high clast concentration, which inhibits particle segregation. The deposits may exhibit clast fabric or imbrication due to the high shear rates that exist at the base of the current (Branney and Kokelaar, 2002).

1.4.2 Turbulent Flow

Fluid turbulence becomes the dominant clast support mechanism when the upward component of the eddy velocity is greater than or nearly equal to the settling velocity of individual particles (Rouse, 1939; Allen 1984). Fluid lift and drag forces both work to keep the particles aloft in the current during transport. Turbulence tends to be the dominant regime in currents where particle concentrations are low (less than a few volume percent) and clast sizes are relatively small. Under these conditions, clast collisions have minimal influence on the dynamics of the current. However, turbulence can also be an important (though not dominant) mechanism of particle support in currents where concentrations are higher, and particle interactions are non-negligible (Branney and Kokelaar, 2002).

1.4.2.1 Particle Support

Particles in turbulent flow are supported because the upward component of the drag force exerted on individual particles due to the turbulent eddy velocities is greater than the settling velocity of the particles. The aerodynamic lift on the particles can be accounted for by one of two mechanisms: the aerofoil effect and the Magnus effect (e.g. Tritton, 1988; Coulson and Richardson, 1990). The aerofoil effect is the same principle by which airplanes acquire their lift force. That is, when a horizontally directed fluid interacts with an inequant particle, a pressure

gradient forms across the oblate clast. This pressure imbalance results in a lift component to the motion of the particle and allows it to remain aloft in the current. The Magnus effect works on particles rotating around an axis that is perpendicular to the primary flow direction. The upper surface of the particle is rotating in the direction of flow, while the bottom surface is rotating against the flow. The result is acceleration of the fluid over the top of the particle and slowing of the fluid below the particle. Again a pressure gradient forms, with a zone of high pressure below the particle and low pressure above, thus resulting in a lift force applied to the particle.

1.4.2.2 Particle Segregation at the Flow Boundary

In dilute (less than a few volume percent), turbulent currents, there is little particle segregation above the base of the current and the flow boundary zone because turbulent eddies are efficient at mixing the current. However due to the polydisperse nature of PDCs, the largest particles in the current may not be fully supported by the turbulent eddies, and as a result they move as a part of the traction population. These clasts are rolled or dragged along the deposit surface. They may be intermittently entrained and re-deposited as turbulent eddies encroach upon the flow boundary zone. When an eddy entrains clasts from the deposit, it does so selectively according to the hydraulic properties of the clasts: size, density, and shape (Li and Komar, 1992). In this way, larger particles may be left behind while smaller, less dense particles are lifted into the current. Once in the current, the largest and densest particles will settle out and deposit first when turbulence diminishes. This results in the deposition of coarse, fines-poor lenses that may also show normal grading. In this way, clast segregation does occur in the flow boundary zone, but it is not as relevant a process in the upper portions of the current (Branney and Kokelaar, 2002).

1.4.2.3 Deposition

Deposition occurs in turbulent flow when the eddy velocities are no longer sufficient to support individual particles. Because currents in which turbulent transport is the dominant mechanism of particle transport are so dilute, clast interactions are unimportant, even during the sedimentation process. Particles can be deposited from a direct-fallout type flow boundary zone, meaning that that the effects of both clast interactions and the upward escape of fluid are negligible (Branney and Kokelaar, 2002). However, if the eddy velocities are such that suspended transport is prohibited but sufficient enough to allow particles to roll or be dragged along the base of the deposit, a traction-dominated flow boundary zone can exist at least intermittently (Middleton and Southard, 1994). A flow boundary zone dominated by traction is more common in PDCs than the direct-fallout because of the wide range in grain sizes typically found within the current. As turbulent eddies encroach upon the flow boundary, traction carpets form from these particles that are momentarily in motion as they are moved along the base. Once the eddy passes, the particles are re-deposited, often showing effects of particle segregation and alignment as a result of being dragged along the base of the deposit.

1.4.2.4 Resulting Deposits

Deposits from turbulent currents tend to be characteristically stratified, diffusely-stratified and/or cross-stratified (e.g. Cas and Wright, 1987; Allen, 1994). The dilute nature of the current allows for impingement of turbulent eddies on the flow boundary zone, and, as a result, the development of intermittent traction-dominated transport of clasts as they are dragged or rolled across the top of the deposit. As the clasts are dragged along the base of the current

there is significant segregation of clast according to size and density. This segregation allows for the development of thin (often diffuse) layers in the resulting deposits. The individual layers can be anything from well to poorly sorted and show either normal or reverse grading.

1.4.3 Fluidized Flow

When currents are highly concentrated, it is possible for conditions to develop in which the effects of the interstitial gas on particles within the current become non-negligible. The gas that fills the pore space between clasts acts to buffer clast interactions and inhibit particle sedimentation. This high pore fluid pressure results in a loss of energy due to particle collisions and lower rates of sedimentation, which allows for increased runout distances in fluidized currents. There are a number of mechanisms by which fluidization may occur (Branney and Kokelaar, 2002).

1.4.3.1 Particle Support

The interstitial gas that provides the high internal pore fluid pressure could have originated from many different sources, with some more likely than others. It is possible that the gas is derived from the substrate and moves upwards through the current resulting in what has been termed *flow fluidization*. This could be due to melting of ice or snow, burning of vegetation, or degassing of underlying pyroclasts; however, it is unlikely that these sources could provide sufficient gas flux over either the spatial or temporal scales on which PDCs can occur (Allen, 1984). *Bulk self-fluidization* occurs due to a significant amount of ambient air being entrained at the head of the current (Walker et al., 1980). This mechanism of fluidization is efficient for both highly concentrated and short-lived, single pulse type flows, but it is not an effective mechanism for currents in which there is a sustained flow of material from the vent. In *grain self-*

fluidization, hot pyroclasts exolve gas during transport, which contributes to the high pore fluid pressure (Sparks, 1978). However, this mechanism for fluidization cannot be the only mechanism by which fluidization occurs because secondary PDCs have been known to occur months to years after emplacement, long after signification exsolution from juvenile material would have ceased (e.g. Rowley et al., 1981; Torres et al., 1996). Finally, fluidization can also occur due to *sedimentation fluidization.* When particles begin to settle towards the base of the current in these highly concentrated conditions, interstitial gas is displaced and forced upwards. The fluxing of gas towards the upper portions of the current exerts a drag force on the particles, resulting in the "hindered settling" of clasts (e.g. Wilson, 1980; Druitt, 1995; Branney and Kokelaar, 2002). Each of these mechanisms of fluidization may play a part in maintaining the high pore fluid pressure necessary to result in the observed high runout distances. In addition, the presence of a high proportion of fine ash will result in decreased rates of pore pressure diffusion. This means that in currents with a significant fine ash fraction, runout distances are even greater because the pore fluid pressure can be maintained longer.

1.4.3.2 Particle Segregation

The effectiveness of particle segregation in fluidized currents depends mainly on the gas flux (Wilson, 1980). In a low gas flux state, the interlocking of particles prevents particle segregation or elutriation of fines. With a moderate gas flux, internal pore fluid pressures are high enough to allow for dilation of the base of the current. This expansion in the basal region results in normal grading of dense lithic clasts and inverse grading of less dense pumice, but the gas flux is still not sufficient to cause high rates of elutriation of fine ash. When a high gas flux exists, bubbling can occur which results in high rates of elutriation, strong inverse grading of

pumice, and potentially the development of fines-poor lithic concentrations near the base of the current (Wilson, 1980). This model of particle segregation based on gas flux ignores shearing within the current, the effects of which are still poorly understood (Branney and Kokelaar, 2002). One other potentially complicating factor affecting particle segregation in fluidized currents is humidity (Hoffmann and Romp, 1991). Low humidity amplifies the electrostatic effects between clasts, and high humidity can result in cohesive behavior of particles.

1.4.3.3 Deposition

Lab experiments have demonstrates that in fluidized flow there is no sharp rheological boundary between the current and the progressively forming deposit (Vrolijk and Southard, 1998). Instead, clast concentration, effective viscosity, and yield strength increase towards the base of the current and continue increasing into the uppermost portions of the deposit. In addition, shear rates decrease to zero at the flow boundary zone. The changes in these parameters that result in deposition occur for three reasons: (1) the gas flux is lower closer to the base of the current due to increased concentrations, resulting in diminished particle support; (2) a decrease in dilation of the flow due to decreased dispersive pressures because of the low shear rates near the flow boundary; and (3) density stratification of polydisperse flows (Branney and Kokelaar, 2002). Rates of deposition are inhibited in a fluidized current because the upward escape of gas as particles settle towards the base prevents the frictional interlocking of clasts (Branney and Kokelaar, 2002). As clasts fall towards the flow boundary zone (or the flow boundary zone rises towards the clasts), they deposit due to interlocking with the substrate because the gas flux is no longer sufficient to allow for the particle to remain in suspension.

1.4.3.3.1 Deposits

Fluidized currents tend to deposit massive lapilli-tuff lithofacies due to the lack of shear at the flow boundary interface. Without shear in the flow boundary zone, tractional segregation does not occur and thus the resulting deposits lack stratification. In addition, the lack of shear on the flow boundary zone inhibits the development of directional fabric or imbrication of clasts (although this may occur to a minor degree) (Branney and Kokelaar, 2002).

The varying gas flux in fluidized currents can result in varying degrees of fines-depletion in the deposits. In the case of low gas flux, deposits may retain a high amount of the fine ash fraction, but where there is significant gas flux, the resulting deposits could be highly fines-depleted. The deposits that result from fluidized currents may also show fines-depleted, lithic rich pods, lenses, or layers due to the high rates of elutriation (Wilson, 1980). Because the deposits can retain a relatively high degree of fluidization even after deposition, elutriation pipes may develop by which gas escaped towards the surface (Fisher, 1979).

1.5 Erosion by PDCs

Despite the many recent advancements in the study of pyroclastic density currents, perhaps one of the most important gaps in our understanding of these currents is the mechanism(s) for substrate erosion and the influence of substrate entrainment on downstream flow dynamics. Erosion by sediment gravity flows has been noted in many natural settings (Rowley et al., 1981; Hungr et al., 1984; Kieffer and Sturtevant, 1988; Benda, 1990; Sparks et al., 1997; Cole et al., 1998; Calder et al., 2000; Stock and Dietrich, 2006; Brand et al., 2011). However, the mechanism(s) for erosion and substrate entrainment, and the impact on downstream flow dynamics, has not been rigorously explored. The fundamental force driving

these flows down-slope is the current's high density relative to the ambient environment; thus, changing the bulk density of the flow via entrainment of the substrate will affect current mobility and runout distance, both of which are important for hazard assessment of these geophysical flows.

Erosion by PDCs has been noted at a number of locations including Mount St Helens, USA (Rowley et al., 1981; Kieffer and Sturtevant, 1988; Brand et al., 2011), Lascar Volcano, Chile (Sparks et al., 1997; Calder et al., 2000), and Soufriere Hills Volcano, Montserrat (Cole et al., 1998). These studies have demonstrated that erosion can take place in a variety of settings. For example, at Mt St Helens Rowley et al., (1981) note up to 35 vertical meters of erosion where the steep flanks meet the shallowly dipping plain surrounding the volcano, scouring from the steep flanks, and Kieffer and Sturtevant (1988) describe longitudinal vortices carved on the downstream side of topographic obstacles. In addition, Calder et al. (2000) attempt to spatially constrain erosion by identifying distinctive basement rock types within the deposits and provide evidence for the widening of previously existing channels and carving of new channels. However, few (if any) field studies have succeeded in determining the location and quantifying extent of erosion, mostly due to limited exposure.

The theoretical and experimental work on granular flows is extensive (see Iverson, 2001 and references therein). There has been a significant effort to examine the mechanisms by which dry granular flows erode and entrain the substrate during granular, rock and debris flows (e.g., Hungr and Evans, 2004; Crosta et al., 2009; Mangeney et al., 2010; Rowley et al., 2011; Estep and Dufek, 2012), and how the dynamics of the system are affected by entrainment of the substrate (Pouliquen and Forterre, 2002; Aranson et al., 2006). Mangeney et al. (2010) showed that entrainment from a thin layer of erodible material at the bed can increase the mobility of

granular flows by up to 40% when the slope of the bed is between the angle of repose for the granular material and the avalanching angle at which surging fronts are able to develop. They also show as the thickness of the erodible bed increases the runout distance of the current increases almost linearly. This result suggests that erosion by these flows is a supply-limited process.

Despite the amount of work that has been done on erosion by granular flows, it is unclear whether the same mechanisms for erosion exist for semi-fluidized PDCs. Fluidization has been known to significantly alter the dynamics that govern the granular system as well as add a high degree of complexity to their understanding (Sparks et al., 1978; Wilson, 1980; Druitt et al., 2007). A series of recent studies by Roche et al. (2002; 2004; 2005; 2008) have shown that initially fluidized granular mixtures share aspects of their behavior with gravity currents of pure Newtonian fluid. These results are important because it emphasizes the range of behaviors that are possible within a granular system based on the level of fluidization.

In order to continue to address the role erosion plays in affecting the dynamics of PDCs, a comprehensive field study is necessary to begin to validate some of the experimental results related to the topic. Until recently, this was extremely difficult due to the lack of sufficient exposures that vary both spatially and temporally. Thanks to thirty years of erosion through the unconsolidated deposits of the May 18, 1980 eruption at Mount St Helens, outcrops with significant evidence for erosion now exist. What follows is the description of a study that attempts to constrain the locations of entrained material throughout the deposits, the sources for that entrained material, and how substrate material may have influenced the dynamics of the current.

Chapter 2

Field evidence for substrate entrainment by pyroclastic density currents and its effect on downstream dynamics at Mount St Helens, Washington (USA)

2.1 Introduction

Pyroclastic density currents (PDCs) are one of the most dangerous volcanic hazards due to their unpredictability, high velocities, and dynamic pressures that can exceed 100 kPa (Valentine, 1998). Because of the difficulty of obtaining direct measurements, volcanologists integrate measurements, observations, and interpretations of deposits with experimental and numerical modeling techniques to understand how PDCs transport material and interact with topography (e.g., Sparks et al., 1976; Branney and Kokelaar, 2002; Roche et al, 2002; 2004; Dufek and Bergantz, 2007), and ultimately to assess the hazards of such phenomenon (Houghton et al., 1987; Orsi et al., 2004).

Two of the most important gaps in our understanding of PDCs are the mechanism(s) for substrate erosion and the influence of substrate entrainment on flow dynamics. The fundamental force driving these flows down-slope is the current's high density relative to the ambient environment; thus, changing the bulk density of the flow via substrate entrainment will affect current mobility and runout distance, both of which are essential for hazard assessment of these geophysical flows.

Erosion by PDCs has been noted at a number of locations including Mount St Helens, USA (Rowley et al., 1981; Kieffer and Sturtevant, 1988; Brand et al., in review), Lascar Volcano, Chile (Sparks et al., 1997; Calder et al., 2000), Peach Springs Tuff, USA (Buesch, 1992), and Soufriere Hills Volcano, Montserrat (Cole et al., 1998). These studies suggest that erosion can take place in a variety of natural settings and under different flow conditions. For

example, Rowley et al., (1981) note that the PDCs generated during the afternoon of the May 18, 1980 eruption of Mount St Helens (MSH) eroded up to 35 vertical meters of material where the steep flanks meet the shallowly dipping pumice plain surrounding the volcano, suggesting that erosion is favored at breaks in slope. Kieffer and Sturtevant (1988) describe longitudinal furrows on the downstream side of topographic obstacles at MSH, carved by the infamous 1980 lateral blast, suggesting that turbulent vortices form due to flow interaction with these obstacles and can aid in erosion. Buesch (1992) describes an increase in the amount of entrained lithic fragments in the Peach Springs Tuff where the currents encountered high surface roughness, suggesting that increased turbulence in the boundary layer can allow for easier entrainment of the substrate. Exposures at Lascar volcano allowed Sparks et al. (1997) and Calder et al. (2000) to spatially constrain erosion by identifying distinctive basement rock types within the PDC deposits and linking them to upstream locations where the distinctive basement lithology is found. These distinctive units are commonly exposed as topographic obstacles and within channel constrictions, thus they suggest that upon entering constrictions in the valley, the PDCs accelerated, allowing the flows to more easily erode the substrate. Despite these important observations, few (if any) field studies have succeeded in quantifying the extent of erosion, primarily due to limited exposure. As such, the mechanism(s) for erosion and substrate entrainment and the impact on downstream flow dynamics have not been rigorously explored through field relationships.

The May 18th, 1980 eruption of Mount St. Helens (MSH) produced multiple, concentrated PDCs, burying the area north of the volcano under 10s of meters of deposits. Thirty years of erosion through these unconsolidated deposits provides extensive outcrops with ample evidence for substrate erosion (Brand et al., in review). Here we present methods and results that

constrain the locations where locally entrained material is present in the PDC deposits, the sources for that entrained material, and begin to explore how substrate material may have influenced the dynamics of the eroding current. We address three main questions related to erosion by PDCs: (1) What are the conditions under which substrate erosion is promoted in PDCs? (2) What are the mechanisms by which erosion occurs (e.g., high basal shear rates, underpressure with the passing head of the current)? And (3) how does substrate erosion (i.e. bulking) and self-channelization due to erosion influence downstream PDC dynamics?

2.2 May 18th 1980 Mount St Helens Eruption – Eruptive events, previous work and hypotheses

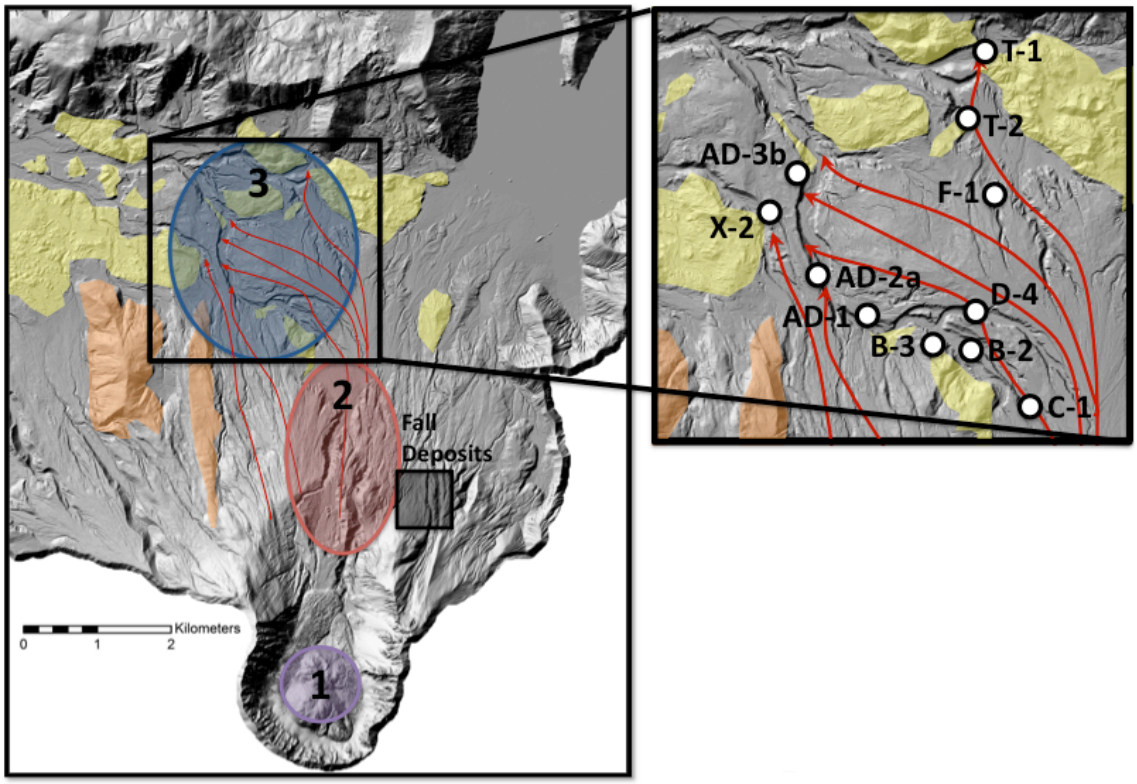

Figure 1. LIDAR map of the Mt St Helens crater north through the pumice plain. Orange regions represent pre-existing topography. Yellow regions represent exposed debris avalanche hummocks deposits. Dotted line represents depositional area of afternoon PDCs. Regions 1, 2, and 3 represent source regions for the PDC lithics, including the vent, flank and debris avalanche, respectively. Black box indicates area from which fall deposits were sampled.

The eruption at Mount St Helens began when the domed, unstable north flank failed, resulting in the largest landslide (debris avalanche) in recorded history (Rosenfeld, 1980). The debris avalanche deposited a series of hummocks that extends across the pumice plain, the area north of the volcano (Yellow shading, Figure 1), and continues up to 24 km down the Toutle River valley (Glicken, 1996). The landslide was immediately followed by the infamous lateral blast, produced due to the rapid decompression of the cryptodome (e.g. Kieffer, 1981; Druitt, 1992). The lateral blast was a dilute PDC that traveled ~30 km to the north, devastating > 450 square kilometers (Bursik et al., 1998). Within a half hour, a Plinian eruption column reached 12 km into the atmosphere, and continued to rise until around noon when the column began to collapse (Christiansen and Peterson, 1981). The afternoon of the eruption was characterized by three PDC producing phases: (1) an early phase as the eruption was building energy, (2) the climactic phase, associated with the peak mass flux and eruptive intensity, and (3) a late PDC phase associated with the waning eruption (Rowley et al., 1981; Criswell, 1987). The afternoon PDCs were more concentrated than the earlier lateral blast (Brand et al., in review) and traveled >8 km north of the volcano depositing up to 40 m of pyroclastic material (Criswell, 1987; Brand et al., in review). The debris avalanche hummocks, scattered across the pumice plain, provided meters to tens of meters of vertical relief, which the afternoon PDCs flowed around and, in some cases, overtopped (Figure 1). The explosive eruption waned during the early evening, transitioning to the extrusion of a lava dome over the next days and months (Moore et al., 1981).

Thirty years of erosion through the May 18th, 1980 pyroclastic deposits has resulted in arguably the best-exposed PDC deposits in the world, including near complete incision through the deposits and laterally continuous outcrops that extend proximal to distal from source. Brand et al., (in review) identify five PDC depositional units from the afternoon of the May 18th

eruption. Units III and IV are the most voluminous of the four units and correlate with the climactic phase of the eruption (Criswell, 1987; Brand et al., in review). Both units are characteristically massive and often enriched in lithic blocks. Unit III is massive, poorly sorted, and shows little to no evidence of elutriation or segregation of lithics or pumice. This observation suggests that the effects of density segregation were largely suppressed due to the highly concentrated nature of the PDC that produced Unit III (Brand et al., in review). Unit IV is fines depleted up to medial distances from source but fines normal thereafter and usually contains a lithic-rich base. Unit IV appears to have been deposited from a less concentrated current, relative to Unit III, in which density segregation of clasts was more efficient and the effects of elutriation were enhanced (Brand et al., in review). Units III and IV were chosen for this study based on their lateral extent, excellent exposures and frequent occurrences of lithic block concentrations.

The lithic blocks found within the PDC deposits could have been derived from one of three possible sources: the vent, the steep slopes of the edifice, or the debris avalanche hummocks. Through granulometry, detailed componentry, and statistical analysis, PDC deposits containing locally derived (i.e. entrained from the hummocks) substrate material can be differentiated from those containing only material from the vent or steep flanks. We first assume that the proportions of lithologies in fall deposits also represent the proportions of lithologies in the PDCs prior to entrainment from any sources other than the vent (Region 1, Figure 1). This assumption relies on the correlation of the fall deposits that were sampled with the PDCs that produced Units III and IV. In order to maximize the possibility of that correlation being accurate, fall samples were taken from the coarsest layer of the fall deposits, which we assume correlates to the time of climactic activity, or the period during which Units III and IV were emplaced

(Brand et al., in review). The primary purpose of the correlation is to provide a suite of lithologies to which all PDC samples throughout the pumice plain can be compared.

We further assume that outcrops in regions of no obvious interaction with debris avalanche hummocks can only contain lithics from the vent (Region 1, Figure 1) or erosion along the flanks (Region 2, Figure 1). PDC deposits downstream from debris avalanche hummocks may contain lithics from all three sources (vent, flank and hummocks). By determining characteristics (grain size data, componentry) of the hummocks and then investigating PDC deposits both downstream and upstream from them, we can see how the PDC deposits changed following interaction with the hummocks. We examine four important ways in which the PDC deposits may be similar (or dissimilar) to the hummocks: median grain size, the ratio of pumice to lithics, the ratio of F2 ash (<62.5 μm) to F1 ash (<1 mm) (F2/F1 ratio), and the distribution of lithologies.

2.3 Methods

2.3.1 Field Methods

PDC sample locations are divided into two categories: those without obvious interaction with debris avalanche hummocks and those that were deposited following interaction with the hummocks. The deposits that were sampled without obvious interaction with debris avalanche hummocks also fall into two categories: the most proximal deposits located between the flanks and the first hummocks (e.g., Outcrops C-1, C-2; Figure 1) and those located just upstream (Outcrops AD-1, AD-3b, F-1; Figure 1) or adjacent to a set of hummocks (Outcrop B-2; Figure 1). Samples taken from upstream or adjacent locations are compared with PDC deposits directly downstream from a given set of hummocks (e.g., Outcrops B-3, X-2, AD-2a, T-2; Figure 1) to see if the grain size distribution, fine ash content, and componentry change to reflect interaction with the hummocks.

Each samples was sieved down to 8 mm in the field and 1 mm in the lab using standard sieving techniques (Walker, 1971). Fractions <1 mm were measured using a Coulter counter LS-100R laser particle-size analyzer. Componentry included (1) classifying lithics of 16 mm (-4Φ) and 8 mm (-3Φ) in size as pumice, basalt, andesite, dacite, and rhyolite; and (2) Classifying 100 lithic blocks (>64 mm) per sample into units from one of four recent eruptive periods (3 ka–present): Goat Rocks, Kalama, Castle Creek, and Pine Creek (see Hausback, 2000 for a full description of the lithologies). It should be noted that while we are confident in our ability to assign each clast to an eruptive period based on hand sample characteristics, what we are really comparing is how the abundances of lithologies changes at different locations.

2.3.2 Chi-Square Test for Homogeneity

The Chi-Square Test for Homogeneity is used to statistically determine evidence for substrate entrainment and constrain the sources of entrained lithics within the PDC deposits at MSH. The Chi-Square Test assesses the probability that two samples are statistically different from each other and can be used to tell whether two samples are derived from the same parent population.

Eisenhart (1935) first suggested the method of applying the Chi-Square Test to quantify lithologic variations; the method presented here has been adapted from their initial description. The following is a demonstration of how the Chi-Square Test has been applied in this study (See Appendix for sample calculation). For the sake of this example, Table 1A shows two samples (S_1 and S_2), the components of which can be separated into two distinct categories (C_1 and C_2), but the table could be modified for any number of samples (S_i) or categories (C_j).

A. Observed	**Categories**		**Total**
	C_1	C_1	
S_1	(S_1C_1)	(S_1C_1)	(S_1)
S_2	(S_2C_1)	(S_2C_1)	(S_2)
Total	(C_1)	(C_1)	N

B. Expected	**Categories**		**Total**
	C_1	C_2	
S_1	$(S_1)(C_1)/N$	$(S_1)(C_2)/N$	(S_1)
S_2	$(S_2)(C_1)/N$	$(S_2)(C_2)/N$	(S_2)
Total	(C_1)	(C_2)	N

Table 1. A. Example of an initial set up with total counts given for each row and column. Parentheses denote summing. B. Table showing how to calculate expected counts for each sample.

To calculate the expected distribution it is assumed that both samples originated from the same parent or source. Under this assumption, the ratio of C_1 to the total in both S_1 and S_2 should be the same. Therefore, the *expected* frequencies are calculated as shown in Table 1B.

The difference, d_{ij}, between the *observed* frequencies given by Table 1A and the *expected* frequencies given by Table 1B is calculated as:

$$d_{ij} = \frac{(S_i)(C_j)}{N} - (S_iC_j)$$

From each of these differences, the Chi-Square Statistic, X^2, is computed:

$$X^2 = \sum_{ij} \frac{(d_{ij})^2}{(S_iC_j)}$$

The lower the value for X^2, the more likely it is that the two samples were derived from the same parent population.

Fisher (1932) determined the probability (p-value), of obtaining a higher X^2 than the one calculated if both samples were in fact derived from the same parent population. If a p-value is above 0.05, the two samples are considered to have originated from the same parent population. Below this significance level, the samples are considered inhomogeneous and thus have been derived from two distinct parent populations. It should be noted that the significance level is not an absolute determining factor; rather, it represents a statistical probability. Therefore, we propose the following qualitative categories based on the quantitative chi-square test to address

the question of whether (and where) entrainment occurred. If the p-value falls above 0.10, negligible local substrate entrainment occurred and lithics were primarily sourced from the vent. Sample with p-values between 0.10 and 0.01, near the significance level of 0.05, represent some degree of mixing due to locally entrained substrate material. Finally, p-values << 0.01 represent significant (upstream) substrate entrainment from a local source. Determining where local substrate entrainment has occurred can be further supported by granulometry data and the ratio of pumice to lithics, as will be discussed below.

2.4 Results

2.4.1 Fall Deposits

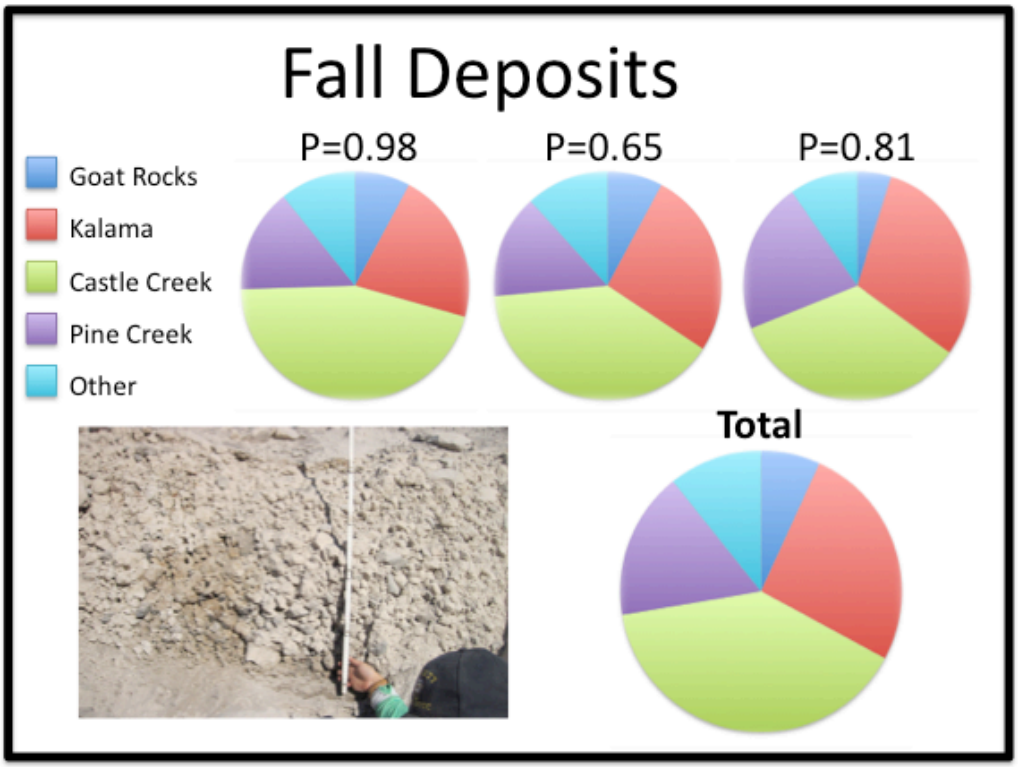

Figure 2. Componentry and P-values for three samples taken from the fall deposit confirming that the lithics all originated from a similar source (the vent). Picture is typical of fall deposits.

The purpose of sampling the fall deposits was twofold: first, to demonstrate the Chi-Square Test for Homogeneity's ability to show that samples we are certain came from a single

source (i.e. only vent erosion) are homogenous and second, to provide a consistent distribution of lithologies to which PDC deposits can be compared. The fall deposits were sampled in three different locations along the same stratigraphic horizon. Each sample was taken from the northwest flank, just to the east of the main drainage exiting the crater to the north (Black box; Figure 1). The samples were taken from the portions of the fall deposit with the largest clasts, both lithics and pumice, to ensure as much as possible that the fall deposits represent the climactic phase of the eruption. In this way, we maximize the possibility that the fall deposits sampled correlate to PDC Units III and IV, which were also produced during the climactic activity. The p-values were computed comparing each sample individually to the other two as well as each sample to the total of the three samples (Figure 2). P-values ranged from 0.65 to 0.98, all well above the significance level, which suggests a steady source of lithics derived from conduit erosion and material collapsing from the crater back into the vent. The distribution of lithic lithologies in the fall deposits is assumed to represent the distribution of lithic lithologies in the PDCs prior to any entrainment from the steep flanks, debris avalanche hummocks, or earlier PDC deposits. The average lithic proportions from the three fall samples are used to assess how the componentry of the PDCs changes once the PDCs began to erode from sources other than the vent.

2.4.2 Debris Avalanche Hummocks

It was noted in Brand et al., (in review) that lithic breccia horizons are often found in PDC deposits directly downstream from debris avalanche hummocks. Thus we hypothesize that the lithic breccia material was eroded from the debris avalanche deposits by the passing PDCs. Four different hummocks (upstream from B-3, AD-2a, X-2, and T-2 in Figure 1) were sampled because they were each exposed in contact with the downstream PDC deposits. Median grain

sizes for the hummocks range from -1.2ϕ to -0.2ϕ, which is similar to PDC deposits throughout the pumice plain (Brand et al., in review). However, the hummocks typically have a bimodal distribution of grain sizes, being dominantly composed of large blocks and fine ash (Glicken, 1996). F2/F1 ratios for debris avalanche hummocks (F2/F1 = <62.5 μm/ <1 mm) are between 0.33 to 0.45, indicating a degree of fines-enrichment that is much greater than the typical PDC deposit (Brand et al., in review). In addition, there was no pumice found in any of the hummocks that we sampled, and the lithic componentry tends to be mono- or bi-lithologic. Kalama Andesite and Castle Creek Dacite are the two most common lithologies present in the hummocks.

If PDC deposits downstream from the debris avalanche hummocks contain locally entrained material, we expect an increase in median grain size due to entrainment of the largest blocks and an increase in the F2/F1 ratios due to entrainment of a matrix that is fines-enriched. We would also expect a decrease in the ratio of pumice to lithics, as any entrainment from the hummocks will result in a dilution of pumice in the PDCs. In addition, the componentry of the PDC deposit is expected to reflect an increase in the lithologies present in the upstream hummock relative to the componentry of the fall deposits.

2.4.3 Pyroclastic Density Current Deposits

As described in the geologic background, lithic breccias are found in three main areas of the pumice plain: (1) proximal to source (Outcrops C-1; Figure 1), (2) downstream from debris avalanche hummocks (Outcrops B-3, X-2, AD-2a, T-2; Figure 1), and (3) as fill facies in channels cut by later PDCs into earlier PDC deposits (AD-3b; Figure 1). We compare (1) the proximal deposits characteristics (e.g., C-1) with the fall deposits to assess if material was eroded from the steep flanks, (2) PDC deposit characteristics downstream from debris avalanche hummocks (e.g., B-3) with the adjacent PDC deposits (e.g., B-2) to assess if material was eroded

from the upstream hummock, and (3) lithic concentrations associated with the PDC channel-related facies with fall to deposits to investigate whether the lithic concentrations in channels were carried the entire way from the vent or if they were locally derived, which has implications for the effect of channelization on flow dynamics.

2.4.3.1 Proximal PDC deposits *between* the steep flanks and debris avalanche hummocks (C-1):

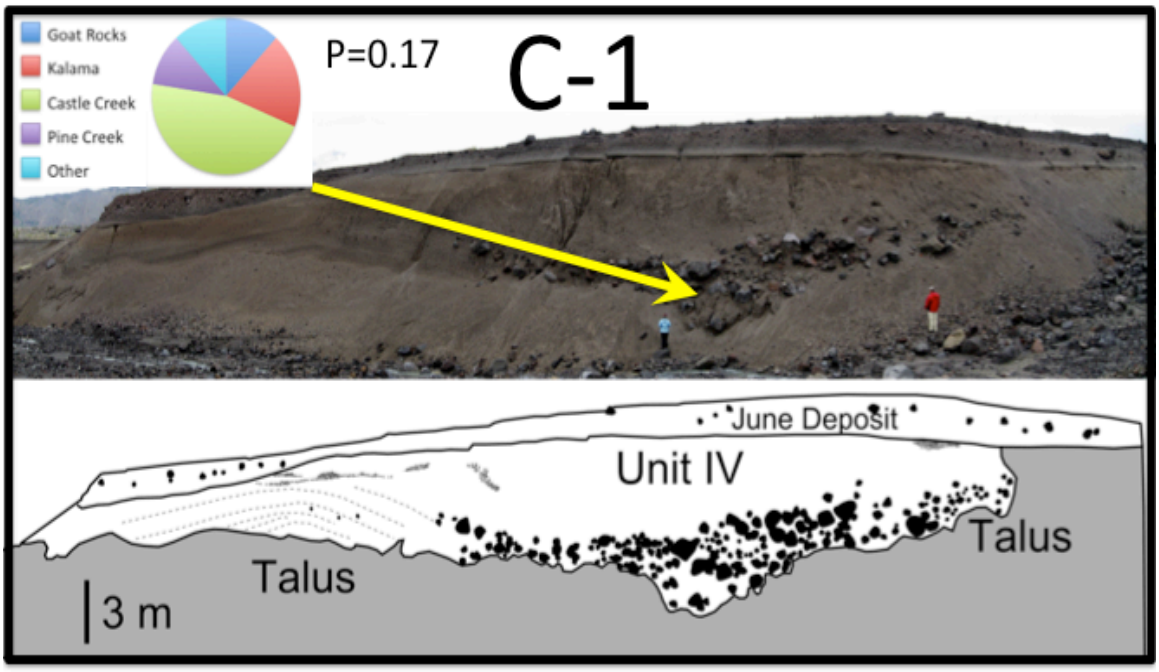

Figure 3. Outcrop C-1 is located 4.8 km from the vent and contains a lithic-rich base, which has a p-value of 0.17, indicating little to no entrained clasts.

Outcrop C-1, the most proximal PDC outcrop located within the pumice plain (4.8 km; Brand et al., 2013), provides an opportunity to examine the characteristics of PDC deposits prior to any interaction with the hummocks because of its location near the base of the steep volcanic cone and upstream from any obvious debris avalanche hummocks (Figure 1). It also allows for a comparison of the componentry here to that of the fall deposits to determine how it has changed during transport down the steep flanks.

The base of the C-1 exposure contains a massive lithic breccia overlain by a massive lapilli tuff. Breccia blocks range in size from 0.64 to 1.2 meters in diameter (Figure 3). The median grain size for the lithic breccia is -6.28 ϕ, the sorting is 3.8, and the F2/F1 ratio is 0.095. While the contact between the PDC deposit and the pre-existing topography is not exposed, regional mapping suggests the lithic breccia represents the base of the fourth and final PDC flow unit deposited during the afternoon of May 18, 1980 (Brand et al., in review).

The lack of exposed hummocks between the volcano and this outcrop suggests that any lithics are derived from a combination of Regions 1 (the vent) and 2 (the steep flanks; Figure 1). We tested this hypothesis by calculating the p-values of the lithic breccia lens in the PDC deposits (Table 2), which is 0.17. P-values above the significance level of 0.05 are considered to be homogenous with a primarily vent-derived source.

2.4.3.2 PDC deposits in contact with debris avalanche hummocks:

2.4.3.2.1 C and B Outcrops:

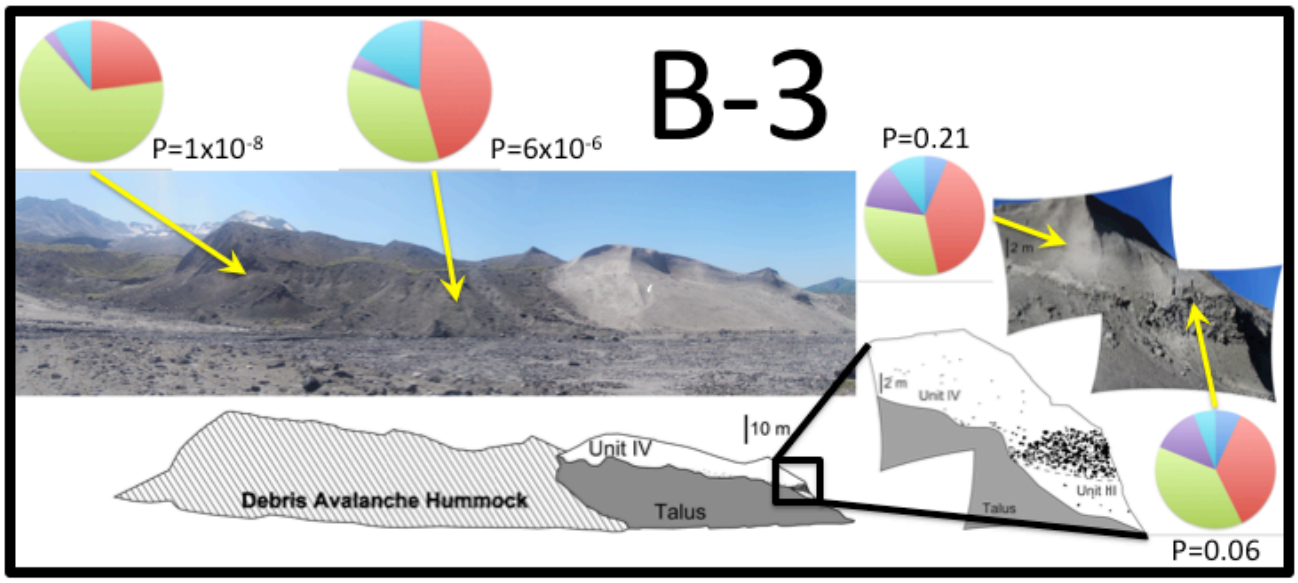

Figure 4. Outcrop B-3 is located 5.3 km from the vent and is located directly downstream from a debris avalanche hummock. The PDC deposit contains a lithic lens that has a p-value of 0.06, suggesting that some entrained occurred from one of the upstream hummocks. For lithology key see Figure 2.

Outcrop B-3, 5.22 km from the vent, is located directly downstream and adjacent to a set of large (>50 m tall) debris avalanche hummocks (Figures 1, 4). Flow direction is roughly left to right as the outcrop is shown in Figure 4. Only Unit IV is exposed at this location. The base of Unit IV is comprised of a discontinuous lithic breccia lens overlain by a massive lapilli tuff. Here we compare samples from the breccia and massive lapilli tuff of outcrop B-3 with those of C-1 and C-2, the latter two having no obvious interaction with debris avalanche hummocks.

The median grain size of the B-3 lithic breccia is -3.8 ϕ and the sorting is 3.4. Blocks in the breccia lens range in size from 0.7 to 1.6 meters in diameter. Although the median grain size for the B-3 lithic breccia is less than that of the C-1 breccia, some B-3 lithic blocks are actually larger than those found in the lithic breccia at C-1. It should also be noted that no lithic breccia was found at the base of C-2, the closest upstream outcrop relative to B-3, further demonstrating the outsized nature of the lithics present in the B-3 lithic breccia. The F2/F1 ratio of the lithic breccia is 0.256, indicating enrichment in the finer ash fraction relative to upstream PDC deposits (F2/F1 ratio for C-1 breccia, is 0.095; Figure 5B). The ratio of pumice to lithics is 0.10 for the 16 mm size clasts and 0.220 for the 8 mm size clasts. The p-value of the lithic blocks is 0.06, in contrast to a p-value of 0.17 for the lithic breccia at C-1. Componentry indicates that the blocks are enriched in Kalama unit relative to the fall deposits (Figures 2 and 4).

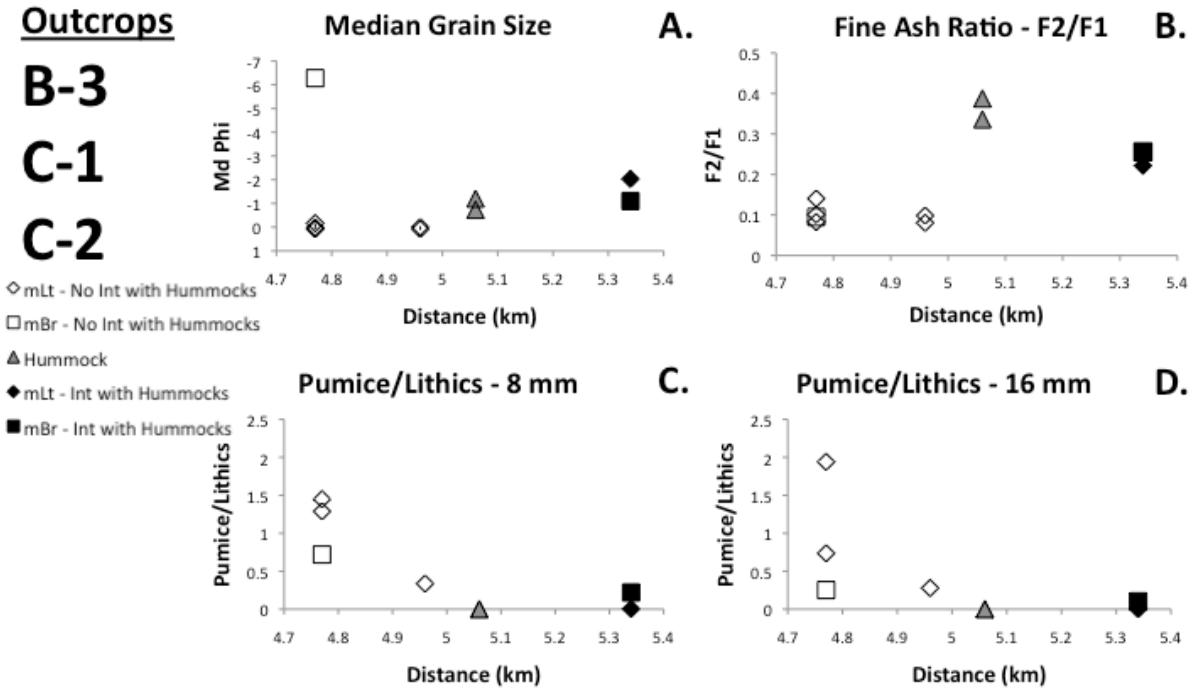

Figure 5. Relative to upstream locations Outcrop B-3 has a higher median grain size (A), higher fine ash ratio (B), and decreased pumice to lithic ratio (C and D).

There is a fairly sharp contact between the lithic breccia lens at the base of Unit IV and the massive lapilli tuff above, which comprises the rest of Unit IV. The massive lapilli tuff has a median grain size of -2.03 ϕ and a sorting of 3.2 (Figure 5A). In comparison, the median grain size of the massive lapilli tuff samples from C-1 and C-2 range from -0.75 ϕ to 0.08 ϕ (Figure 5A) and sorting ranges from 2.7 to 4.0. As such the B-3 massive lapilli tuff has a larger median grain size than other outcrops upstream from this location, with the exception of the lithic breccia at the base of C-1 (Figure 5A). In addition, the B-3 massive lapilli tuff F2/F1 ratio is 0.222, indicating fines-enrichment (Figure 5B) relative to the C-outcrops, which have F2/F1 values that range from 0.08 to 0.19. The B-3 ratio of pumice to lithics (P/L) is 0.00 and 0.003 for the 16 and 8 mm size clasts, respectively (Figures 5C and 5D). These lower P/L ratios indicate a depletion (or dilution) of pumice in comparison with the C-outcrops where the P/L range from 0.25 to 1.94

for 16 mm size clasts and 0.33 to 1.44 for the 8 mm size clasts (Figures 5C and 5D). The p-value for the B-3 massive lapilli tuff is 0.21 (Figure 4).

The upstream hummock was sampled in two locations, 20 meters apart, to observe how the distribution of lithologies in the hummocks changes within short spatial area. The median grain sizes of the two samples are -1.2 ϕ and -0.73 ϕ (Figure 5A) and sorting of 3.6 and 3.83. The F2/F1 ratios are 0.336 and 0.388 (Figure 5B), both indicating a high degree of fines-enrichment. There was no pumice found in the hummocks at this location so P/L ratios were 0.00. The p-values for the hummock are $1x10^{-8}$ and $6x10^{-6}$. While both have extremely low p-values, it should be noted that the two samples taken from the hummock were different from each other in terms of the componentry. One was composed of 45% Kalama and 34% Castle Creek, while the other sample contained 68% Castle Creek and only 23% Kalama (Figure 4).

2.4.3.2.2 X-2 and AD-3a Comparison:

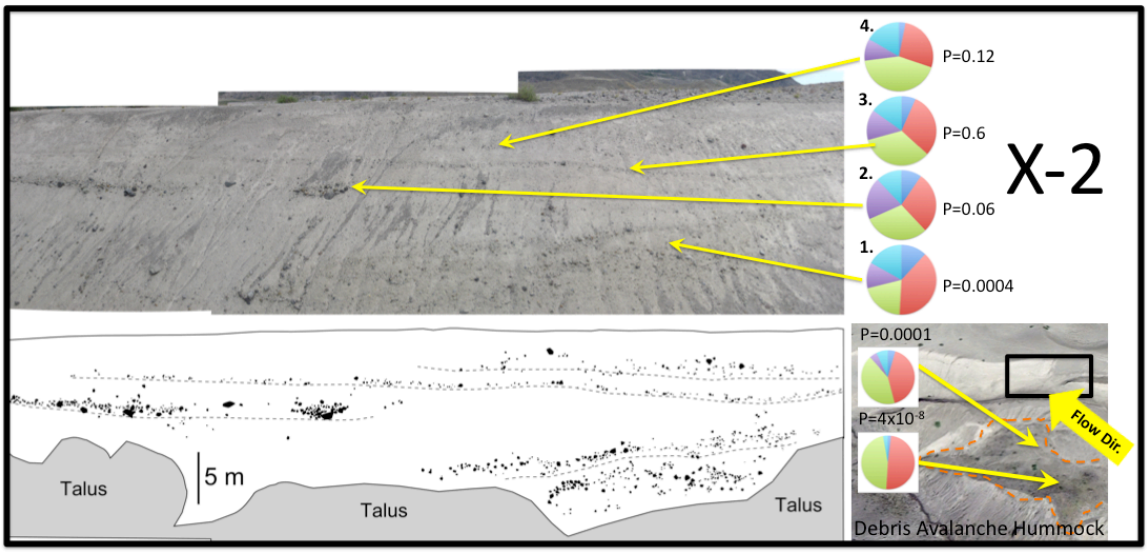

Figure 6. Outcrop X-2 is located 6.1 km from the vent and contains four lithic rich layers. The p-values for the lithics in those layers increases towards the top of the outcrop suggesting that as the pre-existing topography was filled in less entrainment occurred.

Outcrops X-2 and AD-3a are located medial-distal from vent in the western region of the pumice plain (Figure 1). Outcrop X-2 is located 6.12 km from the vent and directly downstream from a series of debris avalanche hummocks that have ~ 3 meters of vertical relief relative to the current surface of the surrounding deposits (Figure 1, 6). Outcrop AD-3a is located northeast of X-2 and, based on the inferred flow lines, is not close to any exposed debris avalanche hummocks (Figure 1; Brand et al., in review). These two outcrops are compared to assess changes in granulometry and componentry that may reflect interaction of the PDCs with the hummock upstream from X-2.

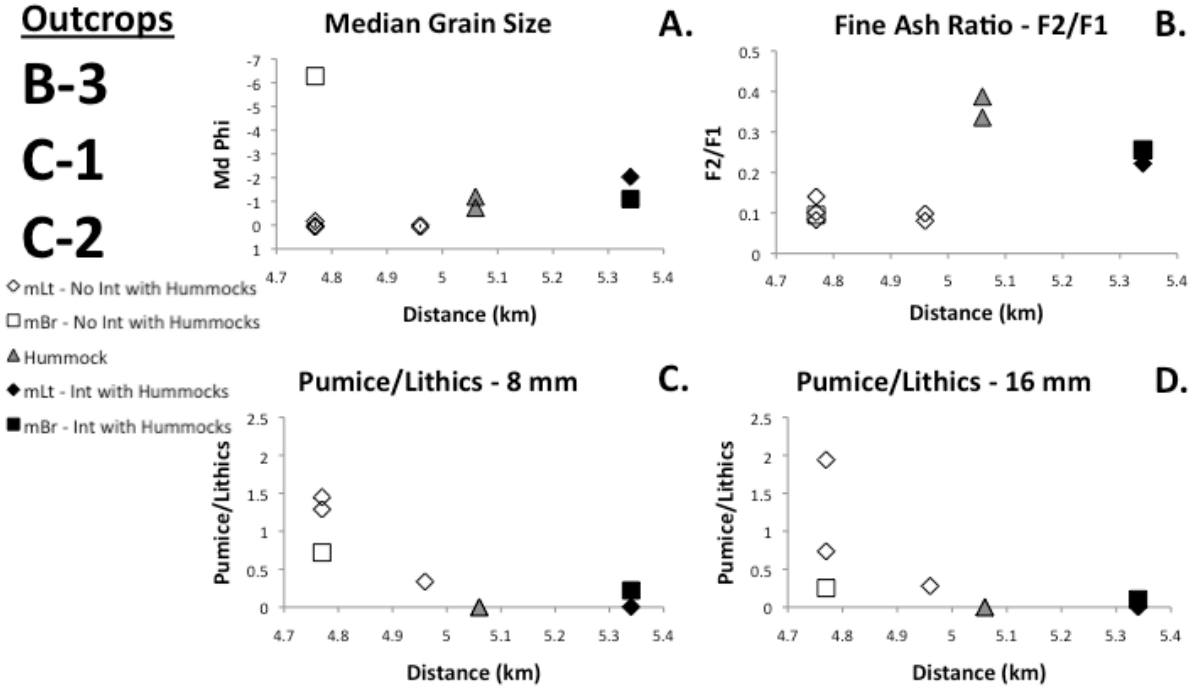

Figure 7. Outcrop X-2, located 6.12 km from the vent and directly downstream from a debris avalanche hummock, (A) has an increased median grain size, (B) increased fine ash ratio, and (C and D) decreased pumice to lithic ratio.

Outcrop X-2 comprises a series of diffuse lithic-rich horizons interspersed with massive lapilli tuff. Due to the lack of continuous exposures from this location to others where the

stratigraphy is well-constrained, it is not possible confidently discern which units are exposed in Outcrop X-2. However, based on relative stratigraphic positioning, they are inferred to represent pulses of deposition from Units III and IV. The median grain size of the lithic rich layers ranges from -2.17 ϕ to 0.8 ϕ (Figures 7A) and the sorting ranges from 3.4-3.98. Blocks in the lithic rich-layers vary from 0.2 to 0.65 meters in diameter. In contrast, the median grain size of the samples from AD-3a range from 0.33 to 0 (Figure 7A), and sorting ranges from 3.17 to 3.29, indicating an increase in grain size downstream from the hummocks at X-2. The F2/F1 ratios for X-2 range from 0.25 to 0.33 (Figure 7B), while for AD-3a the ratios are between 0.22 and 0.26 (Figure 7B), suggesting fines enrichment at X-2 relative to AD-3a. For Outcrop X-2, the pumice to lithic ratios for the 16 mm sized clasts are between 0.005 and 0.26, and vary from 0.05 to 0.5 for the 8 mm sized clasts. These values indicate a dilution of pumice relative to AD-3a, where the P/L ratios range from 0.13 to 0.5 for the 16 mm size clasts and from 0.49 to 0.81 for the 8mm size clasts.

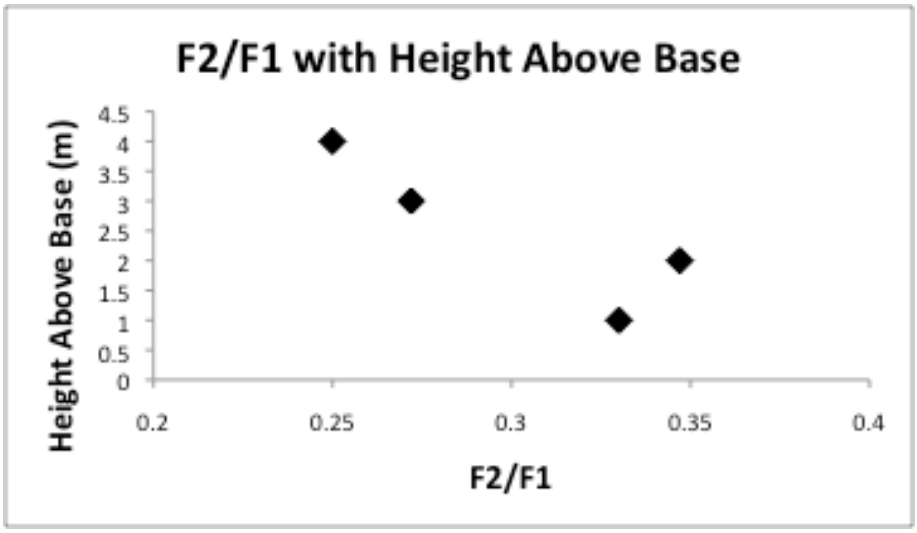

Figure 8. Outcrop X-2 shows a trend of decreasing fine ash ratio with height above the base indicating less entrained material is present in the upper parts of the deposit.

Due to the presence of four distinct and accessible lithic-rich horizons, outcrop X-2 provides the opportunity to examine how the amount of entrained material varies with height in

the outcrop (i.e. as the hummock was progressively buried by PDC deposits). The value for the F2/F1 ratio generally decrease with increasing height above the base, indicating an progressive decrease in fines-enrichment from bottom to top (Figure 8). There is also a general trend of increasing p-values from 0.0004 at the base of the outcrop to 0.12-0.60 toward the top of the outcrop (Figure 6).

The upstream hummock was sampled in addition to each of the four lithic-rich horizons in Outcrop X-2. P-values for the hummock samples are 0.0001 and $4x10^{-8}$ (Figure 6), both well below the significant level of 0.05. Again the hummocks in this area are dominantly composed of the Kalama Andesite and the Castle Creek Andesite, both units making up more than 83% of the hummocks. There was also no pumice present in the hummocks, thus the P/L ratio for the hummocks is 0.00.

2.4.3.2.3 T and F Comparison:

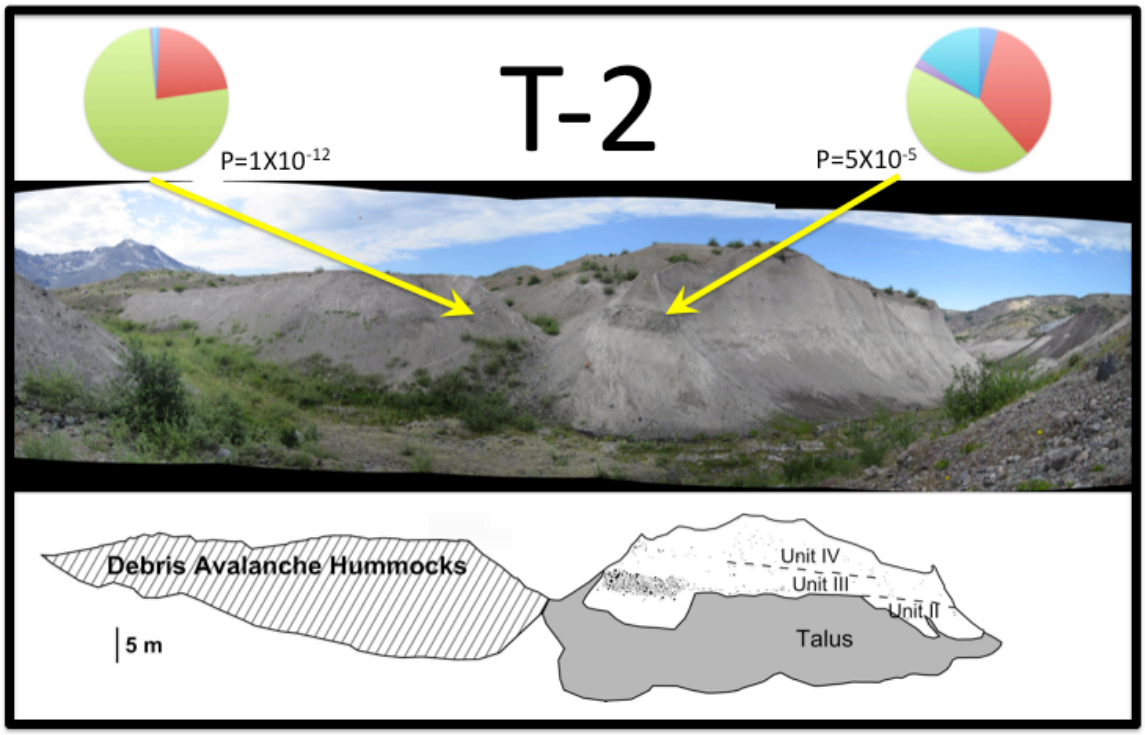

Figure 9. Outcrop T-2 is located 6.87 km from the vent and is located directly downstream from a debris avalanche hummock. T-2 contains a prominent block-rich lens that has a p-value of $5x10^{-5}$ indicating that significant entrainment occurred prior to deposition at this location.

Outcrop T-2 (Figures 1, 9) is located 7.16 km from the vent and directly downstream from a hummock with ~5 meters relative to the current surface of the surrounding PDC deposits. The T-2 outcrops are compared to outcrop F-1, which is located ~500 meters upstream from both outcrop T-2 and the debris avalanche hummocks in this region of the pumice plain. Samples were taken from Outcrop F-1 to determine characteristics of the PDC deposits prior to interaction with the hummocks, and are contrasted with those from T-2, located downstream from debris avalanche hummocks.

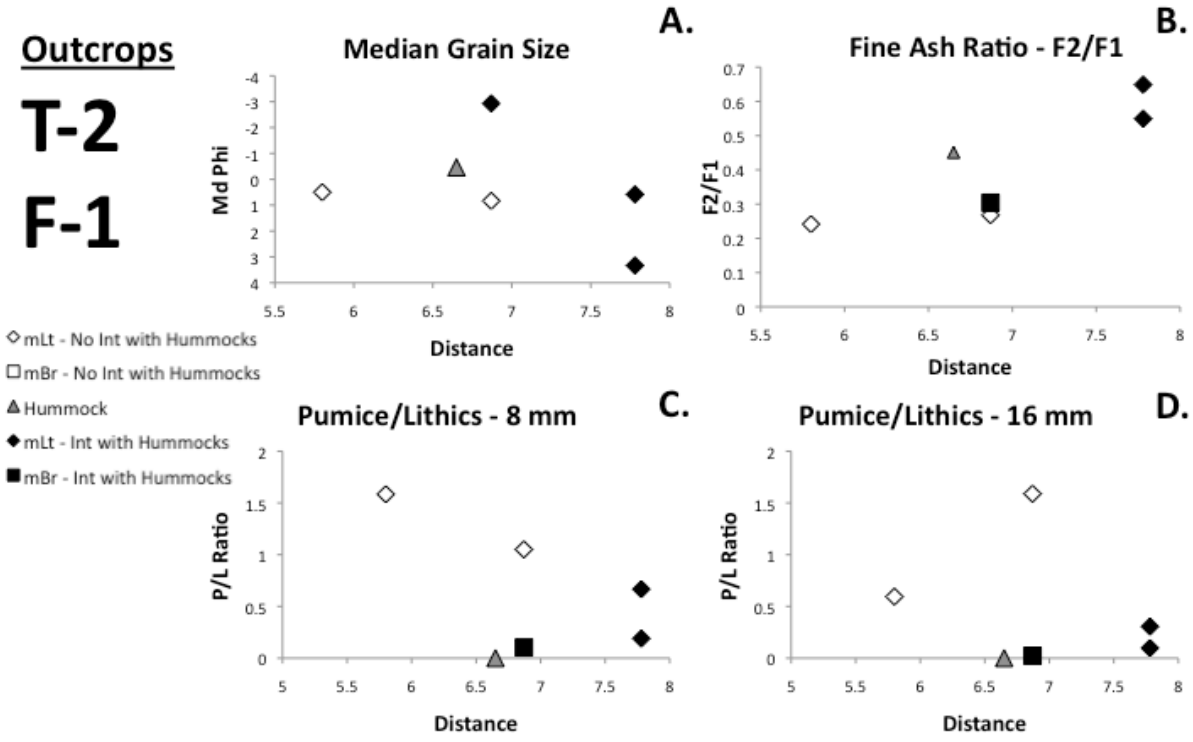

Figure 10. Outcrop T-2, located 6.87 km from the vent and directly downstream from a debris avalanche hummock, (A) has an increased median grain size, (B) increased fine ash ratio, and (C and D) decreased pumice to lithic ratio.

Outcrop T-2 contains Units I-IV (see Brand et al. 2013 for a full outcrop description), but the most significant feature of note is a lithic block-rich lens that occurs at the base of Unit III.

The lithic lens has a median grain size of -2.93 ϕ and a sorting of 3.3. It is composed of lithics that range in size from 0.10 to 0.50 meters in diameter. Samples from Outcrop F-1 have median grain sizes of 0.5 to -1.27, which are much lower than at T-2 (Figure 10A), and sorting values from 2.7 to 3.7. The F2/F1 ratio for the lithic lens at T-2 is 0.31, while at F-1 the F2/F1 ratios range from 0.17 to 0.33 (Figure 10B). While one sample at F-1 has a F2/F1 ratio that is 0.02 higher than that of the block-rich lens at T-2, all other samples fall at least 0.10 below, indicating that the in general T-2 is more fines enriched than F-1. Also, the P/L ratios for the block-rich lens at T-2 are 0.02 and 0.10 for the 16 mm and 8 mm size clasts, respectively. At F-1 the 16 mm size clasts vary between 0.59 and 1.71, while the P/L ratios for the 8 mm size clasts range from 0.76 to 1.58 (Figure 10C and 10D). The samples from F-1 have a much higher concentration of pumice than is found at T-2. The lithic lens in T-2 has a p-value of $5x10^{-5}$ when compared to the fall deposits (Figure 9), which is well below the confidence interval suggesting high amounts of locally entrained material.

The hummock sampled in this location had a median grain size of -0.46 ϕ and a sorting of 4.08. The F2/F1 ratio is 0.45, showing a high degree of fines-enrichment. The debris avalanche hummock has a p-value of $1x10^{-12}$, and the blocks in the hummock are almost exclusively the Kalama (21%) or Castle Creek Andesites (76%) (Figure 9).

2.4.3.2.4 AD-2a:

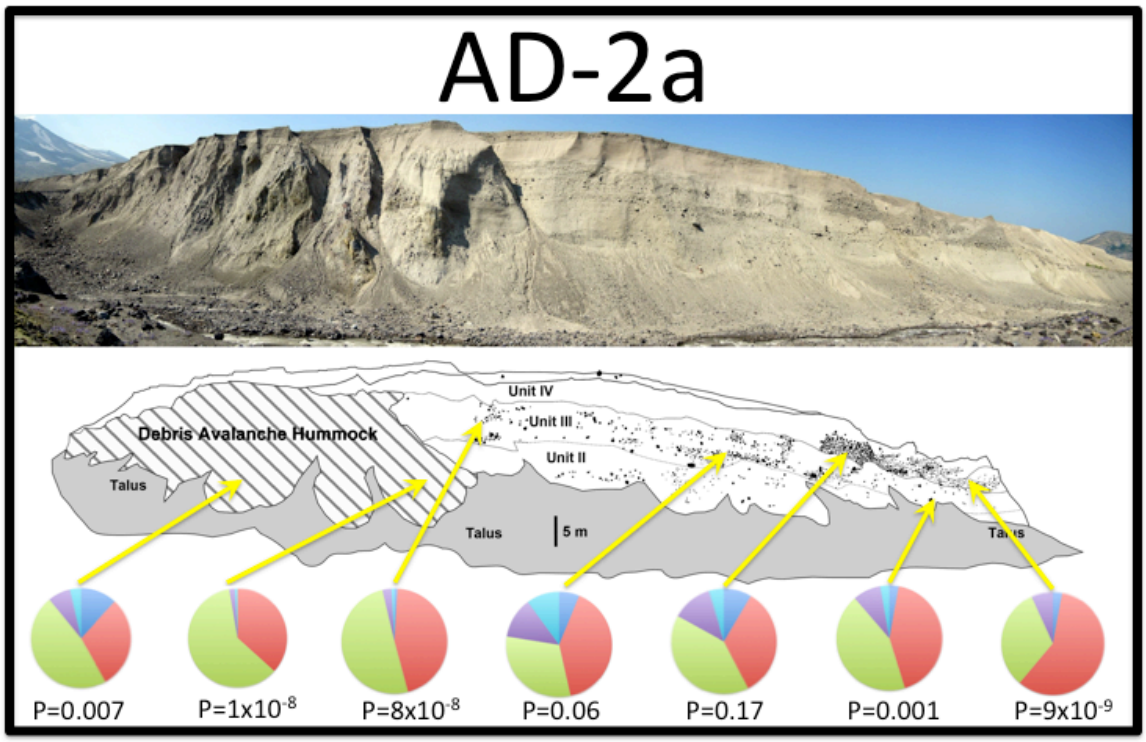

Figure 11. Outcrop AD-2a is located 5.7 km from the vent and contains a number of lithic concentrations as layers, lenses, and pods. The outcrop is highly complex and samples from this outcrop have p-values that range from $9x10^{-9}$ to 0.17 suggesting that in some of the lithic concentrations contain locally entrained material whereas others appear to have been transported from the vent.

Outcrop AD-2a (Figure 1, 11) is located 5.7 km from the vent, north of a set of debris avalanche hummocks. A cross-section through one of the debris avalanche hummocks and the PDC deposits is exposed in the canyon walls, with the contact between the hummock and PDC deposits well-defined (Figure 11). The outcrop is ~40 meters tall and the upstream hummock is approximately the same. Units II-IV are exposed at this location. AD-2a is a complicated outcrop with many block rich layers, lenses, and nested channels. The outcrop is cut nearly north-south, but it is difficult to determine the exact flow direction because it is located near an area where the flows may have been converging from different directions (Figure 1; Brand et al., in review), which could explain the complexity of the outcrop. AD-2a is compared to nearby outcrops AD-1 and AD-2b, neither of which have obvious upstream debris avalanche hummocks (Figure 1).

Although flow directions in this area are complex, these outcrops will roughly allow for a comparison of the PDCs upstream (AD-1), directly downstream (AD-2a) and further downstream (AD-2b) from debris avalanche hummocks.

Unit II is a massive lapilli tuff and is exposed directly against the debris avalanche hummock, and the contact between the hummock and the PDC deposit has an apparent dip of 42°. Unit II pinches out to the north and is the least block rich unit in Outcrop AD-2a, and thus was not sampled for this study. Unit III is marked by a discontinuous lithic rich base, as well as a series of lithic rich concentrations within the unit. The contact between Units III and IV is complex and nearest to the contact with the hummock, it is indicated by a sharp transition from the block-rich Unit III below to the massive, lithic-poor Unit IV above. Approximately 75 meters to the north, the contact abruptly transitions to being marked by a highly block-rich Unit IV above and a less block-rich Unit III below (Figure 11). The contact is scoured in a number of places, particularly below the lithic rich portions of Unit IV further to the north. To the south, near the contact with the hummock, Unit IV is dominated by a block-rich massive lapilli tuff that is relatively featureless and lithic-poor. The massive lapilli tuff quickly disappears to the north, and is replaced by block-rich concentrations, many of which have an arcuate, convex up nature to them. The concentration of lithics decreases to the north of the hummocks, and at the northernmost exposure of this unit it is nearly devoid of large lithic blocks (>64 mm). The convex shape of the block concentrations, combined with the scours below these features, leads us to interpret these features as a series of poorly-developed levees and nested channels.

The median grain size for the block-rich facies in AD-2a is -2.33 and the sorting is 3.29. Median grain sizes range from 0.036 ϕ to -1.57 ϕ and the sorting ranges from 3.27 to 3.41. The grain sizes upstream and downstream do not vary greatly from those found at AD-2a. Upstream

from AD-2a, median grain sizes at AD-1 range from 0.16 ϕ to -1.16 ϕ and sorting varies from 3.02 to 3.69 (Figure 10A). At AD-2b, downstream from AD-2a, the median grain sizes range from 0.51 ϕ to -1.93 ϕ and sorting ranges from 2.60 to 3.66. While there is no significant trend with median grain size, the F2/F1 ratio of samples at AD-2a ranges from 0.199 to 0.362, which are fines-enriched relative to both AD-1 upstream (0.10 and 0.17) and AD-2b downstream (0.10 to 0.14; Figure 11). P-values range from $9x10^{-9}$ nearest to the contact between the PDC deposit and the hummock to 0.17 furthest to the north.

Two samples were taken from the debris avalanche hummock located to the south of Outcrop AD-2a. The p-values of the hummock are both very low, $1x10^{-8}$ and 0.0007, both well below the significant level. As with the other hummocks they are dominantly composed of the Kalama and Castle Creek Andesites.

2.4.3.3 Channelization features with no evidence for upstream hummocks:

2.4.3.3.1 D-4:

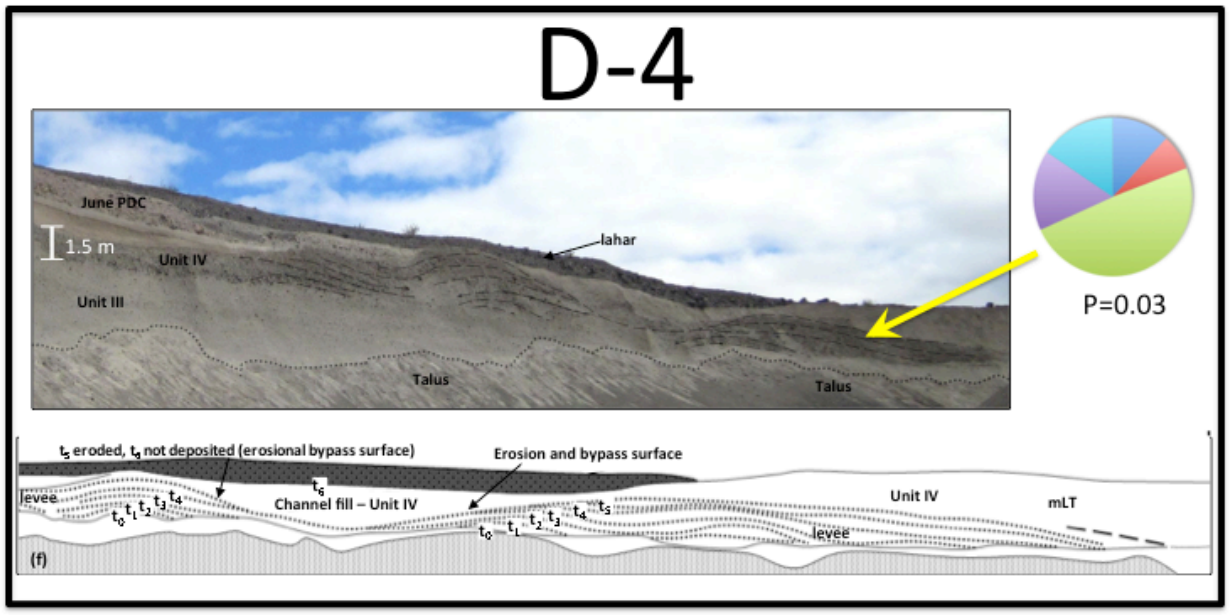

Figure 12. Outcrop D-4 is located 5.55 km from the vent and is not located directly downstream from debris avalanche deposits. Depositional levee features suggest that the PDCs were able to self-channelize, and the p-value of 0.03 indicates that while some entrainment may have occurred from the steep flanks.

Outcrop D-4 (Figure 1, 12) is located 5.5 km from the vent and contains Units II-IV (see Brand et al., in review for full outcrop description). The most prominent features of this outcrop are the lithic levees exposed in Unit IV in both the upstream and downstream walls of the drainage. These levees have been interpreted as a depositional phenomenon expressed as two lithic-rich, convex features in which the interior fabric mirrors the curvature of the upper surface. They levees have been interpret as evidence for self-channelization by the PDCs that produced them (Brand et al., in review). The levee has a median grain size of -3.5 ϕ and a sorting of 3.7. In order to determine whether the levees formed independent of interaction with the hummocks, a sample was taken from this location from the lithic rich levee feature. When compared with the fall deposits, the p-value for the sample is 0.03. This is *below* the p-value significance level of 0.05, which is a proxy for primarily vent-derived lithics.

2.4.3.3.2 AD-3b:

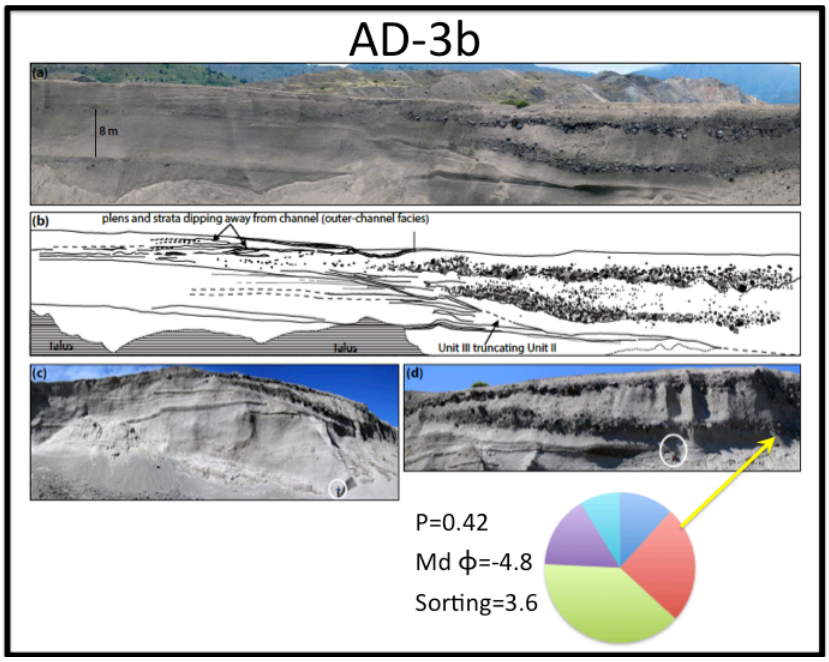

Figure 13. Outcrop AD-3b is located 6.7 km from the vent and contains two channels that have been carved into the underlying PDC deposits. The channels have been filled by a lithic breccia, which has a p-value of 0.42, indicating that the lithics in the breccia have been transported from the vent rather than locally entrained.

Outcrop AD-3b is 400 meters long and located 6.24 km from the vent (Figure 1, 13). Flow lines mapped by suggest this outcrop is downstream from the lithic levees at D-4 (Brand et al., in review). Flow direction is into or slightly oblique (east-southeast to west-northwest) to the outcrop (Figure 1). Units I-IV are exposed here (see Brand et al., in review for a full outcrop description). The two most interesting features of this outcrop are two (nested) erosional channels, carved by the PDCs that deposited Units III and IV. The base of the first channel is the base of Unit III, which carves into the underlying Unit II (Figure 13). The first 2-3 meters of Unit III (within the U-shaped feature) are massive lapilli tuff, but this abruptly transitions into a 0.3 to 1.8 m thick, lithic block-rich layer that extends to the north side of the outcrop where it bends upwards towards the top of the exposure and pinches out. The block-rich layer rapidly transitions into a normal graded, massive lapilli tuff, which thins away from the center of the feature. A lithic block-rich breccia forms the base of Unit IV and overlies Unit III within the channel feature. This block-rich zone grades vertically into massive lapilli tuff. Clasts that comprised the lithic breccia in Unit III range from 0.69 to 1 meter in diameter, and the blocks in Unit IV range from 0.20 to 0.95 meters in diameter. The clasts at this location are outsized relative to nearby outcrops. The median grain size of the block-rich channel fill breccia is -4.8 ϕ and the sorting is 3.6. To determine whether the lithics at this location were locally entrained, as their outsized nature suggests, or carried the entire distance from the vent, a sample was taken from the lithic breccia that makes up the channel fill breccia facies in Unit III (the lithic breccia of Unit IV is inaccessible). The p-value for the lithic breccia in Unit III is 0.42, which is well *above* the significance level of 0.05.

2.4.4 Interpretation of Results:

In general, the debris avalanche hummocks contain a wide range of grain sizes from fine ash to large blocks. F2/F1 values from hummocks average 0.39 Debris avalanche hummocks are also dominantly bimodal in their componentry, containing Kalama and Castle Creek lithologies with p-values far below the threshold indicative of vent erosion. P/L values for the hummocks sampled here are 0. Thus, in examining PDC deposits upstream, adjacent to and downstream from debris avalanche hummocks, we used four pieces of evidence to assess where and under what conditions local erosion and entrainment of the debris avalanche hummocks occurred: an increase in the median grain size, a spike in F2/F1 ratio, a drop in the P/L ratio, and P-values near or below the threshold indicative of primarily vent-derived clasts.

2.4.4.1 Median Grain Size

Outcrop C-1 is the outcrop nearest to the flanks of the volcano, and is located upstream from any debris avalanche hummocks. Therefore, any lithics deposited at this location could have come from either vent erosion or entrainment from the flanks. However, the block-rich breccia at the base of outcrop C-1 has a p-value of 0.17, indicating that little to no entrainment occurred once the material left the vent. This observation suggests that little to no erosion occurred while the PDCs travelled down the steep slopes of the volcano, which contradicts earlier work suggesting significant erosion along the steep flanks of the volcano (Rowley et al., 1981).

For nearly each unit and location, PDC median grain size is greater directly downstream from the debris avalanche hummocks relative to upstream and adjacent PDC deposits. A downstream increase in grain size is counter-intuitive to normal transport processes, which tends

to show decreasing grain size with increasing distances from the vent (Sparks, 1976). However, we interpret this increase in grain size to reflect the entrainment of larger size lithics from the upstream debris avalanche hummocks. Material larger than the median grain size is incorporated into the PDC from the hummock, quickly deposited downstream, and then the grain size continues to decrease away from the local source. This increase in median grain size downstream from the hummocks is observed occurs in outcrops B-3, T-2, and X-2 (Figures 5,7,10).

The only exception to this is Unit III in AD-2a, which shows a trend of decreasing grain size relative to deposits upstream of the hummock, and a slight increase in the median grain size in Unit III of AD-2b. The complexity of the outcrop suggests a complicated depositional environment in which there were flow conversions and overlapping flow paths occurring at the time of deposition.

2.4.4.2 F2/F1 Ratio

Due to the nature of emplacement of the debris avalanche hummocks, they have a strong bimodal distribution of grain size, consisting mainly of large blocks and ash. This ash tends to be highly fines-enriched relative to any PDC deposits, with an average F2/F1 ratio of 0.39 whereas the average F2/F1 ratio of the PDC deposits is 0.22. Downstream from debris avalanche hummocks, samples have an F2/F1 ratio that ranges from 0.25 to 0.35, all above average in terms of F2/F1 ratios. When the locations downstream from hummocks are compared with the upstream and surrounding PDC deposits, every location we sampled throughout the pumice plain shows an increase in the F2/F1 ratio.

One possible explanation for the increase in F2/F1 ratio is that the fine ash is produced due to comminution of pumice as the PDCs encountered areas of high surface roughness. However, Brand et al. (in review) and Manga et al., (2011) show that there is no significant

variation in pumice roundness throughout the pumice plain, suggesting comminution of pumice occurred only in the areas nearest to the vent prior to the onset of deposition in the pumice plain. Because the F2/F1 ratios of all PDC deposits downstream from debris avalanche hummocks fall between the F2/F1 ratio of the upstream PDC deposits and that of the hummocks, we suggest that the most reasonable explanation for the increase in F2/F1 values downstream in PDC deposits downstream from hummocks is incorporation of the fine-rich debris avalanche ash matrix.

2.4.4.3 Pumice to Lithic Ratio

The debris avalanche hummock deposits sampled for this study are completely devoid of pumice; therefore, any incorporation of material from the hummocks into the PDCs is going to result in a dilution of the amount of pumice relative to lithics. With the exception of two samples from Outcrop X-2, every location downstream from debris avalanche hummocks shows a strong dilution of the pumice as shown by the pumice to lithic ratio (Figures X). Often this ratio approaches zero just downstream from the hummock whereas in locations upstream from the hummock the P/L ratio is commonly greater than 0.5.

The two samples from Outcrop X-2 that also show a high P/L ratio were taken from the two uppermost layers in the deposit. The high P/L ratio relative to other locations where substrate entrainment has occurred from the hummocks may reflect a decreasing amount of entrained material as the landscape was progressively filled in. We hypothesize that by the time these two layers high in Outcrop X-2 were being deposited, the upstream hummocks were almost completely buried and thus there was both lower surface roughness that the PDC encountered and a lower supply of lithic-rich material to be entrained. These two factors resulted in less entrainment and thus less dilution of the pumice.

2.4.4.4 Detailed componentry – P-values

The low p-values for all of the hummocks are expected, as the lithics were clearly not derived from vent erosion, but rather are the products of the landslide that initiated the eruption. In general, the lithic breccias within the PDC deposits downstream from hummocks have p-values that fall below or near the significance interval (exceptions will be discussed below), indicating that local entrainment occurred after the PDC mixture exited the vent. The PDC deposits downstream from the debris avalanche hummocks tend to be enriched in the Kalama Andesite and the Castle Creek Andesite relative to the fall deposits, which are also the two lithologies that dominate the componentry of the hummocks. We propose that the increase in these two lithologies within the PDC deposits is due to upstream local entrainment from the hummocks.

In addition, there is a trend of increasing p-values towards the top of Outcrop X-2 (Figure 8) indicates decreasing amounts of entrained material towards the top of the outcrop. This is consistent with the decreasing F2/F1 ratio and increasing P/L ratio with height in the X-2 outcrop, also suggesting a decreased amount of locally entrained material. There are two reasons for this observation that are inherently linked. As the landscape was progressively filled in, the surface roughness produced by the debris avalanche hummocks was also progressively decreasing. In addition the PDCs were burying the source of the material that was being eroded. The combination of decreasing surface roughness and decreasing source material resulted in less locally entrained material as the PDCs filled in the pumice plain, as reflected in the X-2 stratigraphy.

One exception where the p-value seems higher than expected is the massive lapilli tuff above the lithic breccia lens in Outcrop B-3, where the p-value is 0.21. However, this same

sample shows an increase in median grain size, an increase in the F2/F1 ratio, and a decrease in the P/L ratio, all indicating that material was entrained from the upstream hummocks. Because three of the four criteria for whether local substrate entrainment occurred are satisfied, we believe that the higher than expected p-value is simply a statistical outlier that is a product of the probabilistic approach used to determine homogeneity.

The p-values for the PDC deposits at AD-2a clearly indicate material was entrained; however, the number of hummocks upstream from this location and the inference that flows in this area may have been coming from a number of directions makes it difficult to determine the exact source for the additional lithics. The presence of at least one sample location with a p-value above the significant level (0.17) indicates that there may have been portions of the PDC that deposited Unit IV in this location that were not erosive upstream from this location. Despite the complicated nature of this outcrop, it is clear for the majority of block-rich facies that the clasts deposited in those locations were locally entrained from the hummocks.

2.4.5 Outcrops containing channelization features – Interpretation:

The lithic rich breccia lens at the base of outcrop C-1 has a p-value of 0.17, suggesting that little entrainment occurred while the PDC traveled down the steep slopes or across the southernmost part of the pumice plain. However, the p-values for the levees in outcrop D-4 is 0.03, indicating that some substrate entrainment did occur prior to deposition. Relative to the fall deposits, the sample at D-4 is enriched in the Castle Creek Andesite, which is exposed in the wall of the channels that occur where the steep flanks meet the shallowly dipping pumice plain (Hausback, 2000). It is likely that there was some degree of erosion that occurred at this break in slope, as evidenced by an increase in this lithology in the deposits at this location, but it was not significant enough to result in in p-values below the significance level of 0.05 .

The breccia channel fill facies in Unit III of Outcrop AD-3b has a p-value of 0.42, which suggests that little substrate entrainment from the flank or debris avalanche hummocks occurred prior to deposition. This also suggests that self-channelization promoted increased carrying capacity, allowing larger blocks to flow further from the vent. The near- or above-threshold p-values, average F2/F1 ratios and average and P/L ratios for PDC deposits at outcrops C-1, D-4 and the channel fill at AD-3b suggest minor erosion from the steep flank or debris avalanche hummocks prior to deposition. No debris avalanche hummocks are found outcropping along the PDC flow path from the vent and AD-3b, which explains the lack of hummock material in the PDC deposits.

2.5 Discussion

2.5.1 Conditions Promoting Entrainment

2.5.1.1 Effects of Velocity and Acceleration

At Mount St Helens, the similarity of the componentry of the PDC outcrop located nearest to the vent (C-1) to the fall deposits (Figure 3) suggests that little to no material was entrained from the steep flanks of the volcano by the PDCs that deposited in that location. Similarly, the lithics present in the lithic levees at D-4 and the channel fill lithic breccias at AD-3b both indicate minimal degrees of entrainment from the flanks. Rowley et al. (1981) reported highly variable rates of erosion along the steep flanks for various episodes of activity throughout 1980. They state that 35 vertical meters of erosion occurred at the base of the stairsteps region as a result of the PDCs from May 18. They also drove 16 centimeter-long stakes into the bedrock prior to the eruption of smaller volume PDCs (relative to those from May 18) that occurred on August 7, 1980. After the eruption they noted that in some locations up to 4 centimeters of the stakes were exposed above the bedrock, and in others the stakes were completely removed.

While volume estimates for entrained material present in the PDC deposits are not possible, we suggest that our results showing minimal entrainment from the flanks are more consistent with erosion rates on the order of centimeters rather than 10s of meters. It is possible that the location where 35 vertical meters were removed was due to the lateral blast and/or debris avalanche rather than the PDCs that followed later that afternoon.

Experimental results show that when velocities are greatest in granular flows, so too are erosion rates; however, when the flows are accelerating, entrainment does not occur (Mangeney et al., 2010). While these experiments were done using granular flow, it is not unreasonable to assume that the qualitative results are applicable to dense PDCs as well because the behavior in the basal portion of the current may approach that of granular flow (Felix and Thomas, 2004). We interpret the lack of entrained material from the steep slopes of the volcano to suggest that the flows were likely accelerating down the flanks and therefore not erosive, resulting in the similarity of the deposits at C-1, D-4, and AD-3b to the fall deposits.

2.5.1.2 Effects of Surface Roughness

The high frequency with which block-rich facies are present downstream of debris avalanche hummocks initially suggests that there is some link between the surface roughness encountered by the PDCs and the occurrence of lithic concentrations in the downstream deposits. Outcrop X-2 shows decreasing amount of entrained material with increasing height above the base of the exposure as evidenced by the decreasing F2/F1 ratio, increasing P/L ratio, and increasing p-values towards the top of the outcrop. We interpret this decrease in entrained material higher in the outcrop to reflect that as the deposits filled in around the upstream hummocks, the relief relative to the height of the aggrading PDC deposits decreased as well. Thus, as the surface roughness decreased, the amount of entrained material present in the PDC deposits decreased as well. It is also important to note that as the landscape was progressively

buried, the supply of material to be entrained (non-PDC deposits) also decreased. It is likely that the decreasing amounts of entrained material present in the downstream PDC deposits reflects both decreasing surface roughness as well as decreased supply of material to be eroded.

Much work has been done on the interplay between landscape evolution due to infilling of low-lying areas and the effects of surface roughness on PDC transport and depositional processes (e.g. Valentine et al., 1992; Branney and Kokelaar, 2002; Brown and Branney, 2004; Carrasco-Nunez and Branney, 2005; Pittari et al., 2006). These studies have focused on changes in spatial distribution of facies, grain size data, and componentry over the course of one or many large eruptions as the topography is progressively filled. Our work has also tied changes in granulometry and componentry to the amounts of local erosion, adding further complexity to the way in which PDCs interact with topography may be reflected in the resulting deposits.

2.5.2 Mechanisms of Substrate Entrainment

The results of our field study show that the majority of PDC lithic breccia facies containing eroded and entrained lithics from an upstream debris avalanche hummocks occur at the base of units and often only 10s of meters downstream from the inferred point of local entrainment. This suggests that (1) erosion is most vigorous at or just behind the head of the current, and (2) that the entrained blocks do not become well-mixed into the current; rather, they are dragged or carried along the base of the flow and deposited nearby downstream. However, locally entrained material is also present high above the base of the unit contact (>4 meters) and typically further downstream from the debris avalanche hummocks (100s of meters). The presence of the entrained material high above the base, long after the current head passed and significant deposition had already occurred, suggests that entrainment also occurred during the semi-sustained passing of the PDC body.

A number of mechanisms have been proposed by which PDCs can entrain substrate material during transport. Some laboratory flume experiments suggest that the majority of entrainment occurs with the passage of the head of the current (Girolami et al., 2010; Roche et al., 2010; 2013). Girolami et al. (2010) measured the high shear stresses associated with the sliding head of ash flows due to the presence of a thin, highly-sheared basal layer. Also, experiments on both fluidized and non-fluidized granular flows have shown that an underpressure relative to the ambient environment develops due to dilation just behind the sliding head of the current (Roche et al., 2010; 2013). This underpressure has been shown to aid in the entrainment of substrate particles larger than those in the flow itself. As the uppermost, large particles in the substrate are surrounded by the finer particles in the flow, they can be plucked from the static bed and dragged along the flow base. Finer particles continue to percolate into the open pore space in the substrate and basal portions of the current. When flow velocities are high enough, particles can be lifted up into the current and transported downstream (Roche et al., 2013). The combination of high shear stress and underpressure makes the head of the current a favorable environment for substrate erosion. The observation that most of the locally entrained material within the PDC deposits is present at the contact with underlying unit and only 10s of meters downstream from where is was entrained is consistent with erosion from the sliding head of the current. In this model, the current would pass over the hummock and the sliding head would drag or uplift (if velocities are sufficiently high) material into the current only momentarily. The entrained material is not efficiently mixed into the PDC and is therefore deposited only a short distance downstream as lithic-block concentrations, prior to the deposition of any other PDC material.

Experiments by Roche et al. (2008, 2010) have shown that the body of initially fluidized flows is associated with lower shear stresses (relative to the head) and a significant overpressure, both of which would inhibit erosion. However, other experimental results on granular flow suggest that entrainment can continue to occur after the head of the current has already passed the site of erosion (Rowley et al., 2011; Estep and Dufek, 2012; 2013). Rowley et al. (2011) observed shear-derived mixing features experiments using granular material traveling over a colored substrate (Rowley et al., 2011). In these experiments it was observed that the head of the current had already passed before the mixing features developed. While these experiments were run over a smooth bed, it is likely that the effects of shear-derived mixing would only be enhanced by the presence of more substantial surface roughness due to the higher shear stresses that would result. In addition, extreme force localization has been observed in two-dimensional photoelastic experiments due to the development of force chains (Estep and Dufek, 2012; 2013). These force chains can propagate into the substrate and influence substrate entrainment. The strength of the network formed by these force chains has been shown to increase with increasing shear rate for both two- and three-dimensional shearing granular masses (Hartley and Behringer, 2003; Daniels and Behringer, 2005). These experiments have suggested that despite the lower shear stress and relative overpressure in the body of the current, it is still possible (and likely) for entrainment to occur once the head of the current has passed. While the experiments were completed for granular flow, it is possible that similar conditions exist at the base of dense pyroclastic flows (Felix and Thomas, 2004). More work is necessary to determine what effect these force chains may have in PDCs. However, these results are consistent with our observation that entrained material is present high above the basal contact and appears to have been mixed into the body of the current. In this model for entrainment, either shear derived mixing, force

chain networks, or a combination of the two allow for the displacement of material into the current. In addition, higher degrees of surface roughness would only serve to increase the basal shear stress and enhance the likelihood of shear-induced entrainment.

Surface roughness has been shown to promote the development of turbulence in the boundary layer of PDCs (Valentine and Fisher, 1986; Buesch, 1992). It has been suggested that the irregular flow paths due to turbulence allow for free clasts to be more easily entrained from the substrate (Buesch, 1992). While it is possible that the high surface roughness that the hummocks presented to the PDCs resulted in increased turbulence in the boundary layer and thus higher rates of substrate entrainment, the depositional characteristics of increased turbulence are notably absent from the deposits. The units containing the lithic breccias downstream and around the hummocks do not show an increase in features typically associated with the Type 1 deposits (stratified, well-sorted) that were inferred to result from the development of the turbulent boundary layer (Valentine and Fisher, 1986). For this reason, we interpret the increase in entrained clasts downstream from the hummocks to reflect the increase in basal shear that would have resulted from the high surface roughness (Iverson and Denlinger, 2001)

2.5.3 Effects of Channelization

Brand et al. (2013) proposed that the depositional levees in outcrop D-4 and channel scour and fill feature in AD-3b formed independent of interaction with large topographic obstacles. Rather, the features are interpreted to have formed as a result of self-channelization of the flow due to intermittent fluid instabilities and non-uniformity in sheet flow over a relatively uniform surface (Imran et al., 1998; Branney and Kokelaar, 2002). The componentry of these two lithic-rich features confirms this interpretation that the self-channelization occurred independent of interaction with the hummocks. Both samples are fairly similar to the fall deposits (p-values of 0.03 and 0.42) and very similar to each other (p-value of 0.38). This

indicates that while there may have been some entrainment from the flanks, resulting in the slightly lower p-values relative to the fall deposits, there was little entrainment upon entering the pumice plain, as evidenced by the similarity of the componentry at the two locations.

By confirming that the clasts found at outcrop AD-3b were mostly derived from the vent, their outsized nature relative to lithics in nearby locations becomes even more remarkable. Blocks at this location (6.24 km from the vent) are up to a meter in size. The only other location where lithics of this size were found to be vent derived were at outcrop C-1, which was located only 4.8 km from the vent. There are a number of other locations in the pumice plain with similarly sized clasts, but those clasts were shown to have been locally entrained from upstream hummocks. This ability of the current to transport these large clasts at least 30% further confirms numerical models that have shown channelization allows for sustained flow capacity and competence and increases runout distance (Bursik and Woods, 1996).

2.6 Conclusions

Much evidence exists in the May 18, 1980 afternoon PDC deposits at Mount St Helens for the local entrainment of substrate material from the debris avalanche hummocks. Block-rich facies downstream from the hummocks typically contain a larger than expected median grain size, an increased F2/F1 ratio, a decreased pumice to lithic ratio, and componentry that varies greatly from the fall deposits and is frequently enriched in the lithologies found in the upstream debris avalanche hummocks. Based on the distribution of locally entrained material, we suggest that (1) erosion is impeded while the PDCs are traveling down the steep flanks potentially because the flows were accelerating; (2) erosion is promoted in areas of high surface roughness, which can change over the course of an eruption as topography is filled in; (3) entrainment can

occur either during the passage of the sliding head of the current potentially due to high shear rates and underpressure or during sustained flow from the body of the current as a result of shear induced mixing or force chain networks; and (4) channelization can occur independent of the influence of topography and can increase the carrying capacity of the current.

While this work has provided field evidence supporting laboratory results, such as experiments on erosion in granular fluids (Mangeney; 2010; Roche et al., 2008; 2010; 2013; Rowley et al., 2011; Estep and Dufek 2012; 2013), more work is needed to fully understand the controls and consequences of erosion. Experiments looking at entrainment by fluidized and semi-fluidized flows that more closely approximate PDCs are necessary to further develop our understanding of PDC dynamics.

Allen, JRL (1985) Principles of Physical Sedimentology. Chapman and Hall, London

Aranson, IS, Malloggi F, Clement E (2006) Transverse instability in granular flow down an incline Phys. Rev. E, 73,050302(R) 1-4

Bagnold, R.A. (1954) Experiments on a gravity-free dispersion of large solid spheres in a Newtonian fluid under shear. Proceedings of the Royal Society of London. Series A, Mathematical and Physical Sciences, 225, p. 49-63.

Bardintzeff, JM (1984) Merapi volcano (Java, Indonesia) and Merapi-type nuee ardente. Bulletin of Volcanology, 47, 433-446.

Belousov AB, Voight B, Belousova M (2007) Directed blasts and blast-generated pyroclastic density currents; a comparison of the Bezymianny 1956, Mount St Helens 1980, and Soufriere Hills, Montserrat 1997 eruptions and deposits. Bulletin of Volcanology, 69, 701-740.

Benda, L. (1990) The influence of debris flows on channels and valley floors in the Oregon Coast Range, U.S.A., Earth Surf. Processes Landforms, 15, 457-466.

Branney MJ, Kokelaar P (2002) Pyroclastic density currents and the sedimentation of ignimbrites. Geological Society, London, Memoirs, 27

Brantley SR, Waitt RB (1988) Interrelations among the pyroclastic surge, pyroclastic flow, and lahars in the Smith Creek valley during the first minutes of the 18 May 1980 eruption of Mount St Helens, USA. Bulletin of Volcanology 50, 304-326.

Brown RJ, Branney MJ (2004) Bypassing and diachronous depositions from density currents: evidence from a giant regressive bed form in the Poris ignimbrite, Tenerife, Canary Islands. Geology 32, 445-448.

Buesch DC (1992) Incorporation and redistribution of locally derived lithic fragments within a pyroclastic flow. GSA Bulletin 104:193-1207

Bursik MI, Woods AW (1996) The dynamics and thermodynamics of large ash flows. Bull. Volcanol. 58:175-193

Bursik MI, Kurbatov AV, Sheridan MF, Woods AW (1998) Transport and deposition in the May 18, 1980 Mount St Helens blast flow. Geology 26, 155-158.

Calder ES, Sparks RSJ, Gardeweg MC (2000) Erosion, transport and segregation of pumice and lithic clasts in pyroclastic flows inferred from ignimbrite at Lascar Volcano, Chile, J. Volcanol. Geotherm. Res., 104:201-235

Campbell CS (1990) Annual Reviews of Fluid Mechanics, 22, 57.

Campbell CS, Brennen CE (1985) Computer simulation of granular shear flows. Journal of Fluid Mechanics, 151, 167-188.

Carrasco-Nunez G, Branney MJ (2005) Progressive assembly of a massive layer of ignimbrite with normal-to-reverse compositional zoning: the Zaragoza ignimbrite of central Mexico. Bulletin of Volcanology, 68, 3-20.

Cas RAF, Wright, JV (1987) Volcanic Successions (Modern and Ancient). Allen and Unwin, London. 528 p.

Christiansen RI, Peterson DW (1981) Chronology of the 1980 eruptive activity. In: Lipman PW, Wullineaux DR (eds) The 1980 eruptions of Mount St Helens, US Geological Survey Professional Paper 1250, 17-30.

Cole PD, Calder ES, Druitt TH, Hoblitt R, Robertson R, Sparks RSJ, Young SR (1998) Pyroclastic flows generated by gravitational instability of the 1996-97 lava dome of Soufriere Hills volcano, Monserrat. Geophysical Research Letters 25:3425-3428

Cole, P.D., Calder, E.S., Sparks, R.S.J., Clarke, A.B., Druitt, T.H., Young, S.R., Herd, R.A., Harford, C.L., Norton, G.E. (2002) Deposits from dome-collapse and fountain-collapse pyroclastic flows at Soufriere Hills Volcano, Montserrat: In: Druitt, T.H., and Kokelaar, B.P. (eds) The eruption of Soufrierre Hills Volcano, Montserrat, from 1995 to 1999. Geological Society, London, Memoirs 21, p. 231-262.

Coulson JM, Richardson JF, Backhurst JR, Harker, JH (1990) Chemical Engineering (4th edn.) Oxford.

Criswell CW (1987) Chronology and Pyroclastic Stratigraphy of the May 18, 1980, Eruption of Mount St. Helens, Washington, Journal of Geophysical Research 92:237-266

Crosta GB, Imposimato S, Roddeman D (2009) Numerical modeling entrainment/deposition in rock and debris avalanches, Eng. Geol. 109:135-145

Daniels KE, Behringer RP (2005) Hysteresis and competition between disorder and crystallization in sheared and vibrated granular flow. Physical Review Letters 94, 64-70.

Denlinger RP (1987) A model for generation of ash clouds by pyroclastic flows, with application to the 1980 eruptions at Mount St. Helens, Washington. Journal of Geophysical Research, B92, 10284-10298.

Dobran F, Neri A, G Macedonio (1993) Numerical simulation of collapsing volcanic columns. Journal of Geophysical Research, B98, 4231-4259.

Druitt, TH (1992) Emplacement of the 18 May, 1980 lateral blast deposit east-northeast of Mount St. Helens, Washington. Bulletin of Volcanology 54: 554-572.

Druitt TH (1995) Settling behaviour of concentrated dispersions and some volcanological applications. Journal of Volcanology and Geophysical Research, 65, 27-39.

Druitt T, Avard G, Bruni G, Lettieri P, Maez F (2007) Gas retention in fine-grained pyroclastic flow materials at high temperatures. Bulletin of Volcanology 69:881-901

Dufek J, Bergantz G (2007) Dynamics and deposits generated by the Kos Plateau Tuff eruption: Controls of basal particle loss on pyroclastic flow transport. Geochemistry, Geophysics, and Geosystems 8:

Esposti Ongaro T, Clarke AB, Voight B, Neri A, Widiwijayanti C (2012) Multiphase flow dynamics of pyroclastic density currents during the May 18. 1980 lateral blast of Mount St Helens. Journal of Geohpysical Research, doi:10.1029/2011JB009081.

Estep J, Dufek J (2012) Substrate effects from force chain dynamics in dense granular flows. Journal of Geophysical Research, Earth Surface 117: doi:10.1029/2011JF002125

Estep J, Dufek J (2013) Discrete element simulations of bed force anomalies due to force chains in dense granular flows. Journal of Volcanology and Geothermal Research 254, 108-117.

Eisenhart C (1935) A test for the significance of lithological variations. Journal of Sedimentary Petrology 5:137-145

Felix G, Thomas N (2004) Relation between dry granular flow regimes and morphology of the deposits: Formation of levees in pyroclastic deposits. Earth Planetary Science Letters, 221, 197-213.

Fierstein J, Hildreth W (1992) The Plinian eruptions of 1912 at Novarupta, Katmai National Park, Alaska. Bulletin of Volcanology, 54, 646-684.

Fisher RA (1932) Statistical methods for research workers. Edinburgh and London, Oliver and Boyd

Fisher RV (1979) Models for pyroclastic surgers and pyroclastic flows. Journal of Volcanology and Geothermal Research, 6, 305-318.

Freundt A, Bursik M (1998) Pyroclastic flow transport mechanisms. In: Freundt, A., Rosi, M. (Eds.), From Magma to Tephra, Modeling Physical Processes of Explosive Volcanic Eruptions, Vol. 4. Elsevier Science, Amsterdam, 173–231.

Hartley RR, Behringer RP (2003) Logarithmic rate dependence of force networks in sheared granular material. Nature 421, 928-931.

Hausback BP (2000) Geologic Map of the Sasquatch Steps Area, North Flank of Mount St. Helens, Washington. U.S. Geological Survey, Geologic Investigations Series I-2463

Hein, FJ (1982) Depositional mechanisms of deep-sea coarse clastic sediments, Cap Enrage Formation, Quebec. Canadian Journal of Earth Sciences, 19, 267-287.

Hiscott RN (1994) Traction-carpet stratification in turbudiates—fact or fiction? Journal of Sedimentary Research Section A, 64, 204-208.

Hoblitt, R. P. (1986) Observations of eruptions, July 22 and August 7, 1980, at Mount St. Helens, Washington. US Geological Survey, Professional Paper, 1335, p. 1–44.

Hoffman AC, Romp EJ (1991) Segregation in a fluidized powder of a continuous size distribution. Powder Technology, 66, 119-126.

Girolami L, Roche O, Druitt TH, Corpetti T, (2010) Velocity fields and depositional processes in laboratory ash flows. Bull Volcanol 72: 747–759, doi: 10.1007/s00445-010-0356-9

Houghton BF, Latter JH, Hackett WR (1987) Volcanic Hazard Assessment for Ruapehu Composite Volcano, Taupo Volcanic Zone, New Zealand." Bulletin of Volcanology 49:737-751

Hungr O, Morgan GC, Kellerhals R (1984) Quantitative analysis of debris torrent hazards for design of remedial measures, Can. Geotech. J., 21:663-677

Imran J, Parker G, Katopodes N (1998) A numerical model of channel inception on submarine fans, J. Geophys. Res. 103:1219-1238

Iverson RM (1997) The Physics of Debris Flows. Reviews of Geophysics 35:245-296

Iverson, R.M., Denlinger, R.P. (2001) Flow of variably fluidised granular masses across three dimensional terrain 1. Coulomb mixture theory. Journal of Geophysical Research, 106 (B1), p. 537-
552.

Kieffer SW, Sturtevant B (1988) Erosional Furrows Formed During the Lateral Blast at Mount St. Helens, May 18, 1980. Journal of Geophysical Research 93:14793-14816

Li Z, Komar PD (1992) Longshore grain sorting and beach placer formation adjacent to the Columbia River. Journal of Sedimentary Petrology 62, 429-441.

Lowe DR (1976) Subaqueous liquefied and fluidized sediment flows and their deposits. Sedimentology, 23, 285-308.

Lowe DR (1982) Sediment gravity flows: II. Depositional models with special reference to the deposits of high-density turbidity currents. Journal of Sedimentary Petrology, 52, p. 279–298.

Manga M, Patel A, Dufek J (2011) Rounding of pumice clasts during transport; field measurements and laboratory studies. Bulletin of Volcanology 73, 321-333.

Mangeney A, Tsimring LS, Volfson D, Aranson IS, Bouchut F (2007) Avalanche mobility induced by the presence of an erodible bed and associated entrainment, Geophys. Res. Lett., 34, L22401

Mangeney A, Roche O, Hungr O, Mangold N, Faccanoni G, Lucas A, (2010) Erosion and mobility in granular collapse over sloping beds. J. Geophys. Res 115, F03040. doi:10.1029/2009JF001462.

Middleton GV, Southard JB (1984) Mechanics of sediment movement. Short Course Notes: 3. Society of Economic Paleontologists and Mineralogists. Tulsa.

Moore JG, Albee WC (1981) Topographic and structural changes, March-July 1980. In: Lipman PW, Wullineaux DR (eds) The 1980 eruptions of Mount St Helens, US Geological Survey Professional Paper 1250, 17-30.

Nemec W (1990) Aspects of sediment movement on steep delta slopes. In: Colella A, Prior DB (eds) Course grained deltas. International Association of Sedimentology, Special Publications, 10, 29-73.

Ogawa, S (1978) Multitemperature theory of granular materials. Proceedings of the US-Japan Seminar on Continuum-Mechanics and Statistical Approaches to the Mechanics of Granular Materials , p. 208-217.

Orsi G, Di Vito MA, Isaia R (2004) Volcanic hazard assessment at the restless Campi Flegrei caldera. Bulletin of Volcanology 66:514-530

Pittari A, Cas RAF, Edgar CJ, Nichols HJ, Wolff JA, Marti J (2006) The influence of paleotopagraphy on facies architecture and pyroclastic flow processes of a lithic-rich ignimbrite in a high gradient setting: the Abrigo ignimbrite, Tenerife, Canary Islands. Journal of Volcanology and Geothermal Research 152, 273-315.

Pouliquen O, Forterre Y (2002) Friction law for dense granular flows: application to the motion of a mass down a rough inclined plane. J. Fluid Mech 453:133–151 doi:10.1017/S0022112001006796.

Roche O, Gilbertson MA, Phillips JC, Sparks RSJ (2002) Experiments on deaerating granular flows and implications for pyroclastic flow mobility. Geophys. Res. Lett. 29, 40. doi:10.1029/2002GL014819.

Roche O, Gilbertson MA, Phillips JC, Sparks RSJ (2004) Experimental study of gas-fluidized granular flows with implications for pyroclastic flow emplacement, J. Geophys. Res., 109, B10201, doi:10.1029/2003JB002916

Roche O, Gilbertson MA, Phillips JC, Sparks RSJ (2005) Inviscid behaviour of fines rich pyroclastic flows inferred from experiments on gas–particle mixtures. Earth Planet. Sci. Lett. 240:401–414. doi:10.1016/j.epsl.2005.09.053

Roche O, Montserrat S, Niño Y, Tamburrino A (2008) Experimental observations of water-like behavior of initially fluidized, dam break granular flows and their relevance for the propagation of ash-rich pyroclastic flows. J. Geophys. Res. 113, B12203. doi:10.1029/2008JB005664

Roche O, Montserrat S, Niño Y, Tamburrino A (2010) Pore fluid pressure and internal kinematics of gravitational laboratory air-particle flows: insights into the emplacement dynamics of pyroclastic flows. J. Geophys. Res. 115, B09206. doi:10.1029/2009JB007133.

Roche O, Niño Y, Mangeney A, Brand B, Pollock N, Valentine GA (2013) Dynamic pore-pressure variations induce substrate erosion by pyroclastic flow. Geology 41, 1107-1110.

Rose WI (1987) Volcanic activity at Santiaguito volcano, 1976-1984. Geological Society of America Special Papers 212, 17-28.

Rouse, H (1939) Experiments on the mechanics of sediment suspension. In: Fifth International Congress of Applied Mechanics, Cambridge, Massachusettes, 550-585.

Rowley PD, Kuntz MA, Macleod NS (1981) Pyroclastic flow deposits. In: Lipman, P. W. & Mullineaux, D. R. (eds) The 1980 Eruptions of Mount St Helens, Washington. US Geological Survey, Professional Papers 1250:489-512

Rowley PJ, Kokelaar P, Menzies M, Waltham D (2011) Shear-Derived Mixing in Dense Granular Flows. Journal of Sedimentary Research 81, 11-12:874-884

Savage SB (1983) Granular flow at high shear rates. In: Meyer R (Ed.) The Theory of Dispersed Multiphase Flow. 339-358. New York: Academic.

Savage SB (1984) The mechanics of rapid granular flows. Advanced Applied Mechanics, 24, p. 289- 366.

Savage SB, Lun CKK (1988) Particle size segregation in inclined chute flow of dry cohesionless granular solids. Journal of Fluid Mechanics 189, 311-335.

Scott AM, Bridgewater J (1975) Self-diffusion of spherical particles in a simple shear apparatus. Powder Technology, 14, 177-183.

Scott WE, Hoblitt RP, Torres RC, Self S, Martinez ML, Nillos Jr T (1996) Pyroclastic flows of the June 15, 1991, climactic eruption of Mount Pinatubo. In: Newhall CG, Punongbayan, RS. Fire and Mud: Eruptions and Lahars of Mount Pinatubo, Philippines.

Sparks RSJ (1976) Grain size variations in ignimbrites and implications for the transport of pyroclastic flows. Sedimentology 23:147-188.

Sparks RSJ, Wilson L, Hulme G (1978) Theoretical modelling of the generation, movement and emplacement of pyroclastic flows by column collapse. Journal of Geophysical Research 83:1727-1739.

Sparks RSJ, Gardeweg MC, Calder ES, Matthews SJ (1997) Erosion by pyroclastic flows on Lascar Volcano, Chile, Bull. Volcanol. 58:557-565.

Stock, J. D.,Dietrich, WE (2006) Erosion of steepland valleys by debris flows, Geol. Soc. Am. Bull., 118(9/10), 1125- 1148.

Torres, R.C., Self, S., Martinez, M. M. L. (1996) Secondary pyroclastic flows from the June 15, 1991, ignimbrite of Mount Pinatubo. In: Newhall, C.G., and Punongbayan, R.S, (eds) Fire and mud: eruptions and lahars of Mount Pinatubo, Phillipines. University of Washington Press.

Tritton DJ (1988) Physical Fluid Dynamics. Clarendon Press, Oxford. 536 p.

Walker PL (1971) Grain-size characteristics of pyroclastic deposits. Journal of Geology 79, 6: 696-714

Williams H (1957) Glowing avalanche deposits of the Sudbury Basin. Ontario Department of Mines 65th Annual Report, p. 57-89.

Wilson CJN (1980) The role of fluidisation in the emplacement of pyroclastic flows: an experimental approach. Journal of Volcanology and Geothermal Research 8:231–241

Valentine GA (1987) Stratified flow in pyroclastic surges. Bulletin of Volcanology, 49, 616-630.

Valentine GA (1998) Damage to structures by pyroclastic flows and surges, inferred from nuclear weapons effects. J. Volcanol. Geotherm. Res. 87:117–140

Valentine GA, Buesch DC, Fisher RV (1989) Basal layered deposits of the Peach Springs Tuff, Northwestern Arizona, USA. Bulletin of Volcanology 51:395-414

Valentine GA, Fisher RV (1986) Origin of layer-1 deposits in ignimbrites. Geology, 14, p. 146–148.

Valentine GA, Wohletz, K, Kieffer S (1992) Effects of topography on facies and compositional variation in caldera-related ignimbrite. Geological Society of America Bulletin 104, 154-165.

Vrolijk PJ, Southard JB (1998) Experiments on rapid deposition of sand from high-velocity flows. Geoscience Canada 24, 45-54.

Yamamoto T, Takarada S, Sato S (1993) Pyroclastic flows from the 1991 eruption of Unzen volcano, Japan. Bulletin of Volcanology, 55, 166–175